IEEE Access
Multidisciplinary | Rapid Review | Open Access Journal

Received 18 April 2024, accepted 27 May 2024, date of publication 3 June 2024, date of current version 10 June 2024.

Digital Object Identifier 10.1109/ACCESS.2024.3408807

RESEARCH ARTICLE

Machine Learning Approach for Predicting the Solid Particle Lubricant Contamination in a Spherical Roller Bearing

K. RAMESHKUMAR[1], KAVIARASU NATARAJ[2], P. KRISHNAKUMAR[1], AND M. SAIMURUGAN[1]

[1]Department of Mechanical Engineering, Amrita School of Engineering, Amrita Vishwa Vidyapeetham, Coimbatore 641112, India
[2]Taark Equipments Pvt. Ltd., Pollachi, Coimbatore 642002, India

Corresponding author: K. Rameshkumar (k_rameshkumar@cb.amrita.edu)

This work was supported by the Directorate of Extramural Research and Intellectual Property Rights (ER & IPR), Defense Research and Development Organization (DRDO), India, under Grant ERIP/ER/0803740/M/01/1194.

ABSTRACT The statistical relationship between sensor signature features and lubricant solid particle contamination conditions in a spherical roller bearing has been investigated in this study. The influence of particle size and concentration of solid contaminants in lubricant on the RMS parameter of time-domain acoustic emission, vibration, and sound sensor signals are examined. Machine learning algorithms are trained with time domain statistical features derived from sensor signatures to predict the lubricant conditions. Decision trees, bagging tree ensembles, and support vector machines are used to build ML models. Decision Tree models are built using classification and regression tree algorithms with three distinct split criteria, namely gini, towing, and maximum deviance. A bagged tree ensemble model is constructed using the decision tree as a base learner. In the support vector machine, kernel tricking is done to optimize the classification boundaries. Models built using Acoustic emission signature features predict lubricant conditions with better accuracy compared to models constructed using sound and vibration signature features. Feature-level fusion approach is implemented by combining the vibration, sound, and acoustic emission features at the feature level to improve the prediction power of machine learning models. The bagged tree ensemble and support vector machine models, which are trained using fused features, predict lubricant conditions in spherical roller bearings with an accuracy of around 99%.

INDEX TERMS Acoustic emission, condition monitoring, feature level fusion, lubricant solid particle contamination, machine learning, vibration signature analysis.

I. INTRODUCTION

Modern manufacturing sectors rely significantly on automation to improve their productivity and competitiveness. The maintenance of rotating machinery is crucial in an automated environment. Currently, industries are moving towards condition-based maintenance to avoid catastrophic failure of mechanical parts and reduce the cost of maintenance and downtime. Rotary bearing plays a vital role in reducing the friction between rotating machinery's rotating and stationary components. In bearings, over 70% of failures can be attributed to issues related to the lubricant [1]. Improper lubrication and selection of the bearing, wrong mounting of the bearing, and indirect factors such as overload, electrical discharge, vibration, operating the bearing at excessive temperature, material flaws, and manufacturing faults are significant causes of bearing failure. Improper mounting of bearings leads to load imbalance, misalignments, and bearing heating. Improper lubrication factors include running bearings without renewing the lubricant beyond its service life, insufficient lubrication, over-lubrication, and contamination. Lubricant contamination may occur due to the presence of solid particles in the lubricant, improper sealing, and the presence of dirt or burr in the bearing housing. Inadequate

The associate editor coordinating the review of this manuscript and approving it for publication was Yue Zhang.

lubrication results in abrasive wear and accumulates wear particles in the lubricant. An increase in abrasive solid particles due to continuous operation without proper maintenance accelerates the abrasive wear process and results in failure of the bearing [2]. The contaminant particles in the lubricant are lodged between the race and the ball or roller. Due to the load acting on the bearing, the particles cause defects in the ball or roller and races. The containment particles impinge on the surface of the inner race, outer race, and ball or roller and induce stress concentration. Increased solid particle contamination in the lubricant accelerates the rate of wear in the bearing, causing vibration and eventual bearing failure. Solid particles also induce microcracks and generate surface contact fatigue, pitting, wiping, and scoring over the bearing raceway, reducing the bearing life [3].

Catastrophic failure or a reduction in the life of the bearing can be caused by a variety of factors, including the size, type, and concentration of solid particles, the thickness of the lubricant film, and the size of the bearing. The presence of contaminants in lubricants causes a) the oil film to dilute, b) the temperature to rise and reduce the viscosity of lubricant oil, and c) accelerates the wear. In automated systems, it is critical to keep an eye on the lubricant's state in order to prevent lubricant contamination-related failures and to enable condition-based maintenance, which involves replacing the lubricants as needed. Some degree of particle contamination in such systems is often inevitable despite efforts to prevent it [1], [2]. Therefore, the prediction of solid particle contamination in a spherical roller bearing (SRB) is chosen as the main objective of the current study. The SRB is an ideal solution for heavy axial and radial load conditions. SRB can accommodate shaft misalignments and defections and is suitable for many heavy industry applications in conveyor systems, wind turbines, oil & gas, mining, and paper machines.

Health condition monitoring in rotating machinery is essential, as it reduces the machinery's breakdown maintenance and operating costs [4]. Due to the implementation of Industry 4.0, industries are moving towards condition-based maintenance using a sensor-based approach. Intelligent models have been developed to forecast the state of the machinery and the remaining useful life of the mechanical component or system using sensors, such as motor current, vibration, sound, acoustic emission, etc. The development of artificial intelligence (AI) and machine learning (ML) models utilizing sensor signature features can prevent catastrophic failures in mechanical systems and enable prompt replacement or repair of the affected component. Bearings are a critical part of the rotating machinery, necessitating an effective method to detect lubricant conditions in them. Solid particle contaminants in lubricant can damage the bearing contact surfaces, increasing noise, vibration, and temperature levels, resulting in the premature failure of the bearing. It is necessary that for critical operations, real-time monitoring of bearing is essential. Early detection of lubricant failure modes by sensor-based monitoring systems will facilitate the application of condition-based maintenance (CBM) plans. CBM helps to ensure that the bearings and lubricant serve their entire life, avoid catastrophic bearing failures, and allow timely replacement of the lubricant as needed. In this study, the bearing's acoustic emission (AE), vibration, and sound signatures under various lubricant contaminant conditions are extracted. ML models are constructed utilizing sensor signature data to predict the lubricant conditions in an SRB.

II. LITERATURE REVIEW

A significant amount of research is being conducted on the condition monitoring of machine parts to reduce catastrophic failure and maintenance costs and to automate maintenance activity. Sensors, advanced signal processing methods, and ML models are increasingly used for machine condition monitoring. Condition monitoring uses a variety of signatures, including motor current, sound, vibration, and AE [5]. Intelligent models are built to predict the fault conditions based on sensor signature features acquired in a)time domain, b)frequency domain, and c)time-frequency domains. The literature review focuses on a)particle contamination in lubricants and b)sensor-based intelligent approaches to predict lubricant contaminants in bearings.

A. SOLID PARTICLE CONTAMINATION

Solid particle contaminants in rotating machinery primarily result from a) Implanted contamination, b) Generated contamination, and c) Ingested contamination. Solid particles generally present in the lubricant include Fe, Al, Cu, Sn, SiC, and sand. Solid particle contaminants influence surface damage, fatigue, abrasive wear, and vibration in the bearing and its associated mechanical system [6]. Kahlman and Hutchings [7] studied the effect of hard contaminants in a lubricated roller bearing by introducing Titanium and Silica particles as contaminants. From the wear studies made, it is observed that premature failure of bearings is noticed due to fatigue or abrasive wear. Khonsari and Booser [8] reviewed the detrimental effects of particle contamination in hydrodynamic bearings with particle size and hardness of the particle as the focus. In an experimental investigation, Wang et al. [9] studied the raceway defects in roller bearings caused by solid particle contamination in lubricant oil. They noted that particle contamination causes stress concentrations, which shortens the bearing's fatigue life. Nikas [10] reviewed the particle contamination in bearings, gears, seals, mechanisms, and machines. Scanning Electron Microscope (SEM), Ferrography, and Spectrographic studies conducted by various researchers to identify particle size and shape were discussed in their review. Debris reported in their studies include 'Cu' particles of size 30μm, silicon particles of size 25μm, and Fe particles of size 3–20μm. It was observed that the use of correct filtering systems improved the machine element wear and reduced the premature failure of bearings.

Beghini et al. [11] observed that wear particles, namely Fe, Al, Cu, Sn, and SiC, are present in the various bearing lubricants of size 0-250μm. Solid particle contamination in a

ball bearing was reviewed by Singotia and Jain [12]. In their article, analytical, numerical, and experimental methods were reviewed and various solid particle contaminant materials affecting the bearing's performances were investigated. In a study, steel particles were introduced into the grease lubricant in SRB by Lin et al. [13] to induce wear. Their investigation revealed that lubricant film thinning, and wear debris growth are influenced by grease contamination. The survey by Ding et al. [14] highlighted the possible application of flexure joints based on compliant mechanisms to eliminate the need for lubrication and minimize friction. They explored mechanical design, kineto-static modeling, functional mechanisms, and other recent advances in the development of compliant micro-positioning stages. In rotary bearings, solid particle contaminants in the lubricant lead to noise, vibration, and acoustic emissions. Studies show that lubricant conditions and bearing failures can be predicted well in advance by examining sound, vibration and AE signatures [10], [15], [16], [17].

B. VIBRATION-BASED APPROACHES

One of the well-established methods for locating fault conditions in rotating machinery is vibration-based analysis. Tiboni et al. [16] provided a thorough analysis of vibration-based techniques for machine condition monitoring. In their study, they reviewed the literature on vibration, AE, and other sensor-based approaches to investigate solid particle contamination. Particles of silica and ferric oxide are found in the lubricant used in the ball bearings of electric motors. According to their research, vibration levels rise with increasing concentration and particle size. Frequency spectrum analysis using vibration signatures was carried out by Maru et al. [17] to study the effect of solid particle contamination on vibration levels in a ball bearing. Their investigation demonstrated that the lubricant's increased levels of solid particle contamination caused an increase in vibration levels. Studies on lubricant contamination in roller bearings were carried out by Hariharan and Srinivasan [20] using lubricant mixed with silica particles of varying sizes and concentrations. In this investigation, the lubricant conditions were examined using the vibration signature's RMS values. In a study by Mahajan and Utpat [21], dolomite powder was introduced as a contaminant to the lubricant. In the experiments, a range of particle sizes and three different concentration levels were used to investigate deep groove ball-bearing wear. As part of their investigation, they performed frequency spectrum analysis using the RMS value of the vibration signals. According to their analysis, bearing wear rises as solid particle concentration and size increase. Koulocheris et al. [22] added steel and corundum particles of various sizes and concentrations as contaminants in lubricant grease. They performed vibration analysis to investigate the wear and fatigue life of ball bearings. The impact of particle size and hardness of the particles on the life of the bearing were analyzed in their study. Healthy and defective ball bearings were studied using vibration signatures by Kulkarni and Bewoor [23]. Vibration parameters, namely RMS, Peak and peak to peak, and kurtosis were used to characterize the bearing defects. Nabhan [24] conducted experimental research on deep groove ball bearings to investigate the vibration behavior utilizing both numerical and experimental methods. It was observed that there is a strong correlation between the degrading conditions of slew bearing and various vibration features, including the Lyapunov-Exponent (L-E), Approximate-Entropy (A-E), impulse-factor (I-F), and margin-factor (M-F) [25].

In a deep groove ball bearing, vibration RMS value and peak amplitude parameters significantly influence the solid particle contamination and concentration. Coal particles of size 150 micrometers (μm) with concentrations of 30% and 40% by the grease weight were used to induce contamination in the lubricant [26]. Sheriff et al. [27] studied the ball-bearing performance by contaminating the lubricant using green sand of particle sizes of 75, 106, and 150 μm. Vibration signature analysis was carried out using the RMS parameter. It was observed that vibration parameters have a strong correlation with the lubricant contaminant conditions. The lubrication conditions in SRBs were ascertained by Jacobsen et al. [28] with the use of a MEMS microphone. Their investigation involved the use of grease as a lubricant. A simple linear regression model developed with statistical features was used to estimate lubricant viscosity conditions. It is observed from the literature that the solid particle size and concentration in lubricants influence the vibration levels of rotating elements. Statistical feature information extracted from the vibration signature can be correlated to the condition of the lubricant used in rotating elements such as bearings. Many studies focused on the RMS parameter of vibration signature for identifying good and contaminated lubricant conditions.

C. ACOUSTIC EMISSION SIGNATURE ANALYSIS

AE sensors are widely used to detect the early failure modes and their mechanisms in rotating machines. Tandon and Choudhury [29] examined the techniques for AE measurement to find rolling element-bearing flaws. It is observed that AE methods can identify faults in rotating machinery much earlier than vibration-based approaches [29], [30], [31], [32], [33], [34]. Many studies have been done using AE sensors to monitor lubricant conditions in different types of bearings. Mirhadizadeh et al. [35] have investigated the effects of operational variables, such as load, speed, and oil film thickness, on AE parameters in a hydrodynamic bearing. Taura and Nakayama [36] investigated the lattice structure of the material during the onset of sliding friction using AE based approach. Friction, wear, corrosion, phase transition, cavitation, cracking, fracture, and other changes in the material's state can all be detected using AE sensors. Piezoelectric elements in AE monitoring have a frequency range of 100 kHz to 400 kHz. In this frequency, minor variations due to cracks or subsurface damage can be effectively identified

by the AE sensor. The vibration-based accelerometers capture vibration frequency from 0.5 Hz to 15 Hz. Vibration sensors are unsuitable for detecting early failure modes due to minor cracks or sub-surface damages. Vibration sensors will capture the environmental noise along with noise due to failure modes, which needs to be filtered for further analysis. AE offers a distinct advantage in identifying solid particle contamination in lubricants due to its ability to capture the failure modes much earlier than vibration-based sensors.

Sheriff et al. [37] conducted research on the impact of green sand contamination in ball bearings using contaminant particle sizes of 75, 106, and 150 μm. Experiments were conducted in a grease-lubricated ball bearing at various speeds and load circumstances. AE parameters viz. RMS, kurtosis, and peak-peak were considered in their analysis. Their experiments revealed a strong relationship between wear patterns and AE parameters as a result of solid particle contamination in the lubricant. Schnabel et al. [38] studied plastic deformation in rolling element bearings using AE signatures at higher speed ranges. Their study concluded that the dominance of transient force signals at higher speeds prohibits particle contamination detection. Whereas under low-speed conditions, plastic deformation is effectively captured by AE. Martin-del-Campo et al. [15] continued the work by Schnabel et al. [38] using a similar experimental setup and investigated particle contamination in rolling element bearing using the AE approach. A novel dictionary learning approach was used in their study to detect particle contamination under high speeds up to 3000 rpm. Lubricant starving conditions in an angular contact bearing were predicted using a K-nearest neighbors (K-NN) based classifier trained using an AE signature [39]. Konig et al. [40] monitored wear in a sliding bearing system using AE sensor signals. Experiments were carried out with the addition of 5 mg/l of ultra-fine dust (ISO-MTD-A1) to the bearing lubricant. A deep neural network (NN) was used to classify anomaly detection, particle contamination in lubricant, and inadequate lubrication. Poddar and Tandon [41], [42] studied solid particle contamination using vibration and AE signatures in journal bearing. Silica particles of sizes 10, 30, 50, and 70 μm were used in their experimentation. Results were analyzed based on AE RMS, AE Energy, and AE spectrum amplitude parameters at different concentrations of the contaminants and particle size. In their study, AE frequency characterization for normal and contaminant conditions was identified, and AE RMS and AE energy and vibration parameters were observed to increase with the particle's size and concentration. Cavitation, particle contamination, and oil starvation were studied using AE signature features, and a Weighted K-NN model was developed to predict fault conditions in a journal bearing. Scheeren, Kaminski, and Pahlavan [43] proposed a novel method for health monitoring in low-speed roller bearings using AE signals. They introduced a waveform-similarity-based clustering approach to effectively identify consistent AE sources indicative of wear and localized defects in the raceway. They observed increased degradation rates after 70,000 cycles on a run-to-failure experiment. Their findings indicate that cross-correlation-based clustering techniques are effective in isolating and identifying faults in low-speed roller bearings.

Compared to vibration-based sensors, AE sensors can predict the failure modes much earlier. Limited studies were made to study the lubricant contaminant conditions in rotating elements such as SRBs.

D. MOTOR CURRENT SIGNATURE ANALYSIS

Researchers have attempted to study bearing faults using Motor Current Signature Analysis (MCSA). Onel et al. [44] studied the outer raceway defect in the ball bearing using motor current signature with the aid of Fast Fourier Transform. Alwodai [45] studied the motor bearing using MCSA and identified baseline, outer, and inner race fault conditions using modulation signal bi-spectrum (MSB). An electrical impedance technique was suggested by Maruyama et al. [46] to monitor the lubricant level in deep-groove ball bearings. In order to forecast the lubricant's state, their study estimated the lubricant film thickness and breakdown-ratio. Nakamura and Mizuno [47] recently studied bearing faults using ML approaches with features extracted from MCSA. MCSA has numerous advantages, viz. a) non-invasive, b) does not require special sensors, and c) is suitable for online monitoring. Mainly, MCSA has been performed to study the faults in induction motor bearings where grease is commonly used as a lubrication medium. Motor current signatures were mainly utilized to identify the faulty condition of ball bearings. There is ample scope to use the motor current signature as a source to identify the lubricant contaminant conditions in rotating elements.

E. MACHINE LEARNING APPROACHES USING SENSOR SIGNATURES

In a preventive maintenance activity, machines or components are periodically monitored to identify early fault or damage conditions. Maintenance will be carried out to repair or replace the parts of the system when the fault condition is identified. In some critical machines, continuous monitoring of the machine or process is required. In such situations, sensors-based monitoring is being adopted to identify failure modes and remailing useful life of the component or system. Computational methods and signal processing are needed to interpret the sensor data and ascertain the machine's current state. Off-late, the ML approach is being increasingly implemented for real-time monitoring by building an intelligent model that will predict the machine's condition based on the input sensor signature. Intelligent models are commonly built using ML algorithms to forecast fault conditions based on statistical features acquired from the sensor signatures in time, frequency, or time-frequency domain.

Adamsab [48] reviewed the use of ML algorithms in machinery-bearing fault identification. Various ML approaches, namely support vector machines (SVM),

artificial neural networks (ANN), Decision Trees, K-NN, relevance vector machines (RVM), and support vector regression (SVR), applied to bearing fault identification, have been presented in their review. Studies have been made to identify bearing fault conditions using various sensor signature features [49], [53] using conventional and deep learning approaches. Ni et al. [54] proposed a novel scheme to estimate the remaining useful life for rolling element bearings. A novel health indicator has been proposed by them. A GRU network was employed in their study to predict the RUL of bearing. Poddar and Tandon [42] used AE signature as an input to a machine-learning algorithm to classify cavitation, contamination, and oil-starvation in a journal bearing. They accomplished this by applying ML approaches like K-NN and Decision Trees. It was concluded in their study that ML models can be used to develop online monitoring systems for critical equipment. Wakiru et al. [55] reviewed lubricant condition monitoring, focusing on various traditional and intelligent methods for providing maintenance decision support for machinery maintenance. Recently, Rahman et al. [56] reviewed recent advancements in the application of ML techniques in the oil and lubrication industry. Sugumaran and Ramachandran [57] classified the fault conditions in a roller bearing using SVM and PSVM approaches. Senthilnathan et al. [58] conducted a comprehensive review of recent advancements in fault diagnosis of SRBs. The study discussed various decomposition methods for signal processing and feature extraction, models for analysis of oil-air lubrication and thermal, optimal strategies for sensor placement, and the application of neural networks. They emphasized the application of signal processing techniques such as the discrete wavelet transform (DWT), specifically leveraging Daubechies four with five-layer decomposition for assessing bearing defect severity. Additionally, Orthogonal Fuzzy Neighborhood Discriminant (OFND) features were also explored. Convolutional neural networks (CNN), Bayesian neural networks (BNN), and probabilistic neural networks (PNN) were highlighted as the most popular neural network techniques. Moreover, modified CNN architectures were found to provide high accuracy and robustness, even in noisy conditions.

Sahu et al. [59] studied the solid particle contamination in a roller bearing using a vibration signature. Their study used Silica particles of size 37μm to contaminate the lubricant. Deep learning techniques and SVMs were employed to forecast the conditions of lubricant oil. Their investigation concluded that ML algorithms could reasonably predict the presence of solid particle contaminants in a rolling element bearing. It is possible to apply the suggested methodology to other kinds of bearings, including cylindrical, self-aligning, and tapered bearings. Zhao et al. [60] investigated fault diagnosis methods in rolling element bearings, with a particular focus on oil debris monitoring and abnormal wear detection. They introduced nonferrous contaminants of high hardness in the lubrication to accelerate pitting and spalling in the rolling bearing-rotor test rig. They found that rather than relying solely on vibration signals, incorporating synchronous temperature and oil debris monitoring data helped improve the accuracy of the bearing health assessment. They employed various ML algorithms, such as SVM, KNN, and Decision Tree, which demonstrated good accuracy by incorporating oil debris-based and vibration-based features.

F. SUMMARY OF LITERATURE REVIEW

Based on existing literature, it is observed that solid particle contaminations in lubricants reduce the life of the bearing due to fatigue and abrasive wear [1], [2], [3], [4], [6], [7], [8], [9], [10], [11], [12]. Most of the studies in lubrication contamination detection are focused on offline methods. The use of AI and ML-based techniques in predicting the lubricant conditions is limited in the literature. Developing AI-based techniques is vital for lubricant condition monitoring due to the emergence of Industry 4.0. The literature indicates that while existing studies have investigated ML approaches for detecting particle contamination and predicting the lubricant condition in bearings, many of the studies either employed a single sensor modality or focused on a limited range of particle sizes and concentrations. This potentially limits the robustness and generalization capabilities of the developed ML models. Off-late, sensors have been used to predict the lubricant contamination using the statistical parameters of vibration and AE signature. Some studies use ML models trained on the individual features of vibration, sound, and AE to predict the lubricant conditions. The feature-level fusion approach utilizing the multiple sensors' signature features may improve the reliability of ML models.

In order to predict lubricant conditions in SRBs, the current study focuses on developing ML models that use sound, vibration, and AE signature features separately and simultaneously by fusing the feature data at the feature level, thereby combining the strengths of the three sensor modalities. It investigates a range of solid particle contaminant sizes between 5μm and 100μm, with different concentrations and operating speeds. Few studies in the literature have investigated lubricant condition prediction for SRBs using ML approaches while considering different particle sizes, concentrations, and operating speeds. The present study seeks to address this gap and contributes to the development of robust ML models capable of predicting SRB lubricant conditions across a wide range of operating scenarios. The proposed models can be implemented to achieve CBM strategies for industrial practice.

III. OBJECTIVES AND METHODOLOGY

A. OBJECTIVES

Based on the thorough literature review, research gaps were identified. The objectives are framed by carefully studying the research gaps. The methodology is defined based on the objectives of this project. The important research objectives are listed as follows:

- Establish an experimental setup to capture the AE, vibration, and sound signatures of lubricant conditions in an SRB with varying solid particle contaminant sizes and concentrations.
- Acquire sensor signatures of various lubricant conditions, extract statistical features, and establish a statistical correlation between lubricant conditions and sensor signature features.
- Build ML models for predicting the lubricant conditions and improve the prediction ability of ML models by fusing the sound, AE, and vibration features at the feature level.

B. METHODOLOGY

An experimental setup was established to acquire signatures of AE, vibration, and sound from the various conditions of lubricants in an SRB with varied speed conditions. The vibration and sound signals are acquired using a free-field-array microphone and a tri-axial accelerometer, respectively. AE signature is captured with the aid of a piezoelectric-AE sensor. The 'Vib-pilot' Data Acquisition System (DAS) is used to acquire and digitize the sound and vibration signatures. PC1-2 muti-channel AE board and "AE-Win" software are used to generate AE waveforms, extract features, and analyze AE data. Fig. 1 illustrates the methodology used in this investigation to forecast lubricant contamination in a bearing.

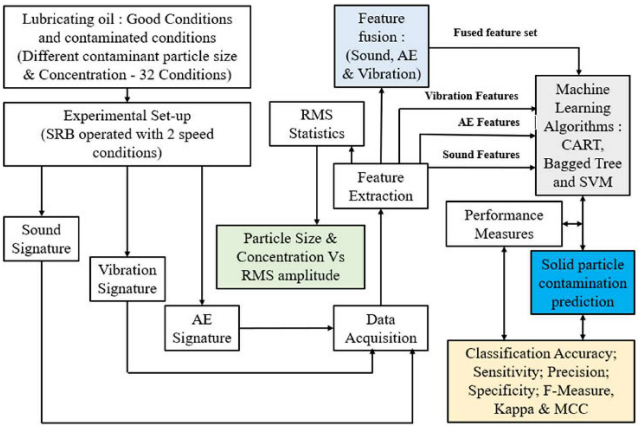

FIGURE 1. Methodology.

C. EXPERIMENTAL SETUP AND DATA ACQUISITION

The experimental setup established in this study is shown in Figures 2 and 3. Fig. 2 shows the line diagram of the experimental setup. A photograph of the experimental setup is given in Fig. 3. The bearing of specification 21308E (SKF) has been used in this study for lubricant condition monitoring by operating the bearing with and without lubricant contamination. The bearing has an outside diameter of 90 mm, a bore diameter of 40 mm, and a width of 23 mm. The radial internal clearance of SRB with the cylindrical base is 100μm (max). The bearing's static and dynamic loading ratings are 108kN and 107kN, respectively. The SRB's outer ring provides four lubrication holes for the recirculation of the lubricant. In this investigation, lubricant oil 'LMTH68', which has an operating temperature range of -20 °C to 100°C, was selected. Base oil viscosity (ISO-VG) is 68 mm^3/s at 40°C and 9 mm^2/s at 100°C. The split plumber block supports the bearing.

D. CONTAMINANT SOLID PARTICLE SIZE AND CONCENTRATION

Experiments are carried out by contaminating the lubricant with 'Fe' and 'SiC' particles. Iron (Fe) particles of size 5, 10, 37, 74, and 100 μm (P1, P2, P3, P4, and P5) are chosen for the experiment. SiC particle of size 10μm is chosen. Experiments are conducted with three different levels of solid particle concentrations, viz. 5%, 10%, and 15% (C1, C2, and C3) at different size of solid particles. The details are shown in Table 1. The total oil required for a single test condition is around 25ml. Fresh oil is mixed with solid particles of the required size and concentration for every test condition for the experimentation. The bearing is operated at two different speeds, 800 and 1200 rpm.

A total of thirty-two lubricant conditions (LC) are established for conducting the experiments. The details are provided in Table 2. Experiments are carried out for 100 sec for every condition. AE, vibration, and sound signature data are acquired by fixing the set sampling rate using the DAQ system. The sensor signals are captured after running the experimental setup for a few minutes to stabilize the lubricant condition. The bearing is flushed with fresh lubricant to remove the contaminants after every experiment and relubricated with the required quantity of lubricant.

TABLE 1. Contaminant particle concentration.

No.	Concentration (%)		Iron Powder (g)	Silicon Carbide Powder (g)	Total Weight (g)
1	C1	5	0.99	0.11	1.1
2	C2	10	1.98	0.22	2.2
3	C3	15	2.97	0.33	3.3

IV. SENSOR SIGNATURE ANALYSIS AND FEATURE EXTRACTION

A. DATA ACQUISITION

In this study, experiments are carried out with thirty-two different test conditions. A triaxial 3273A2 accelerometer is used in this study to capture vibration signatures. Vibration signature is acquired with a sampling rate of 8192 data points per second. Experiments were carried out at every lubrication condition for 100 sec. A Micro30D AE sensor is used to acquire the AE for different lubricant conditions during the experimentation. The operating frequency range of the AE sensor is 150-400 KHz. A sampling rate of 1024 data per hit is chosen to acquire the data. The total number of data points acquired per second is 10,240. Experiments were carried out

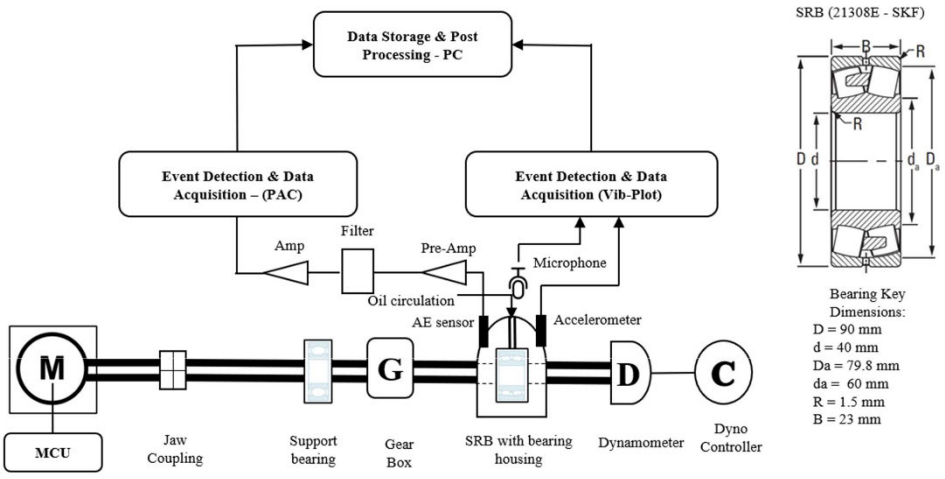

FIGURE 2. Schematic line diagram of the experimental setup.

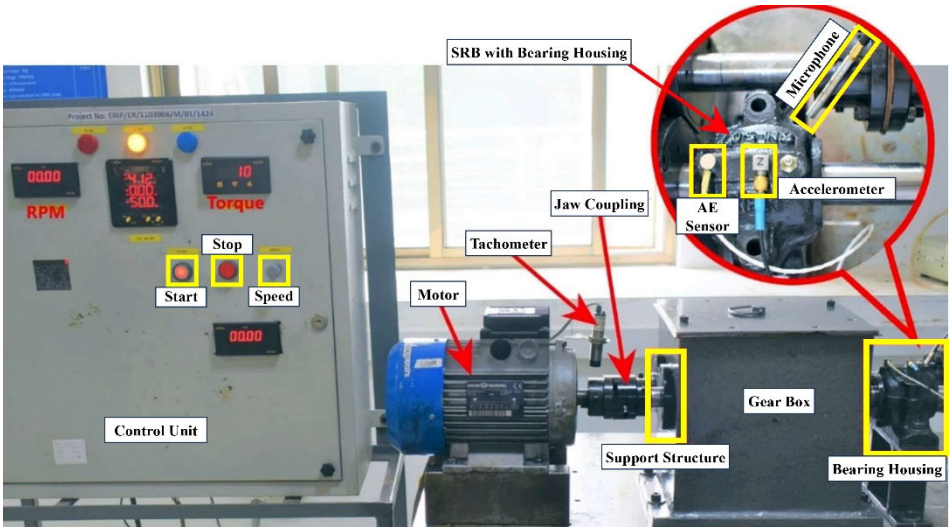

FIGURE 3. Experimental setup photograph.

at every lubrication condition for 100 sec. In order to acquire the sound signature for various lubricant conditions, a GRAS 40PH-10 CCP Free-field Array Microphone was employed in this study. The sound signature is acquired with a sampling rate of 8192 data points per second. A 'Smart Office' analysis software analyses the vibration and sound data. An acoustic emission sensor is also connected to the bearing housing. AE data the sensor captures is sent to the pre-amplifier, and a dedicated AE-DAQ device acquires the signature. An 'AEWin' software is used to analyze the data further. A threshold of 40dB is fixed for AE data acquisition. The data is collected at a fixed waveform sampling rate of 1 MSPS. AE, vibration, and sound measurement chain is illustrated in Fig. 4.

B. SENSOR SIGNATURE STATISTICS

Time domain RMS data were plotted and shown separately for bearings operated at 800 rpm and 1300 rpm for all lubricant conditions considered in this study. RMS of signatures were computed and plotted for 80 seconds. The sensor signatures of the bearing operated with fresh lubricant without any solid particle contamination are shown in Fig. 5. Conditions LC1 and LC2 indicate that the bearing operated with speeds of 800 and 1300 rpm, respectively. The signatures are unique for low-speed (LC1) and high-speed (LC2) conditions in the case of vibration and AE signatures. It is difficult to differentiate the LC1 And LC2 conditions with ease in the case of microphone signatures. The mean statistic of RMS is computed to understand the behavior of sensor signatures at different speed conditions. In the case of AE, for the LC1 condition, the mean is 0.34, and for the LC2 condition is 0.39. for sound signature, the mean value of RMS is 37.40 for LC1 and 38.20 for LC2. For vibration signature, the mean RMS for LC1 and LC2 are 3.57 and 5.12, respectively. It can be concluded that speed conditions could be identified by computing sensor signature statistical parameters when the

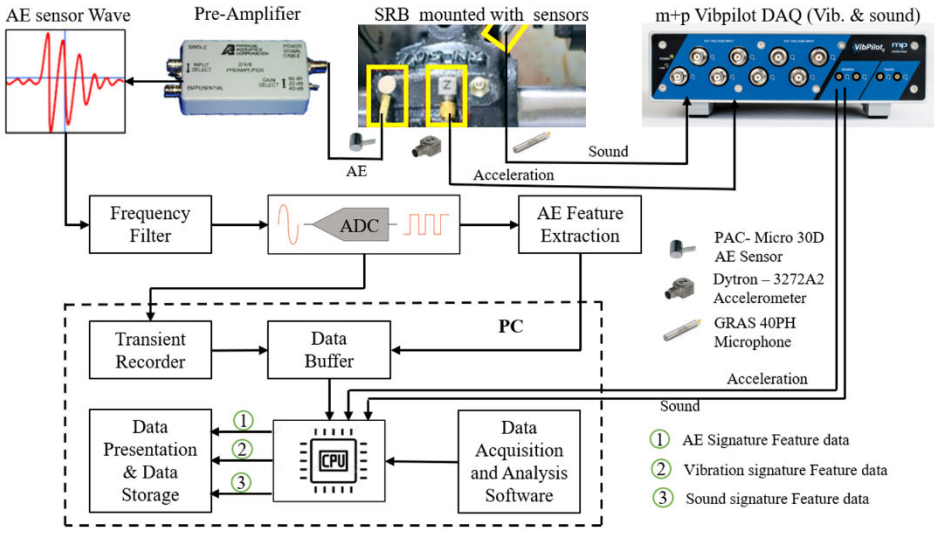

FIGURE 4. AE, Vibration, and Sound signature measurement chain.

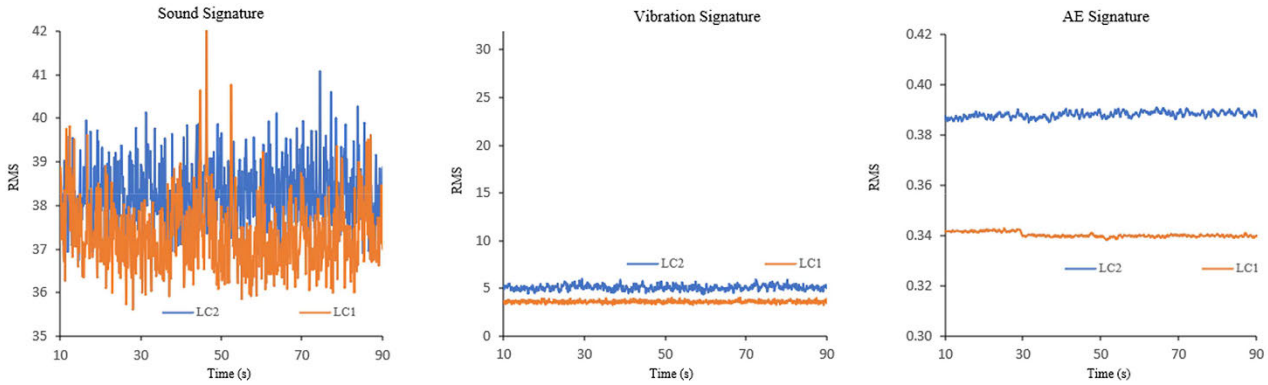

FIGURE 5. Sound, vibration, and AE signatures of Lubricant Conditions (LC1 and LC2)- Fresh lubricant without solid particle contamination. Note: LC1- SRB operated under 800 rpm using fresh lubricant without any solid particle contamination; LC2- SRB operated under 1300 rpm using fresh lubricant without any solid particle contamination.

bearing is operated under lubricant without any contamination.

Signature analysis is carried out for lubricant conditions (LC3 – LC32) with solid particle contamination. Fig. 6 displays the sensor signature patterns for lubricant conditions LC3–LC32. RMS signatures of lubricant have unique patterns for every lubricant condition. It is observed that in the case of sound and vibration signatures, it is challenging to differentiate conditions with ease. In AE signature plots, it is understood that different lubrication conditions have unique signatures and can be distinguished without much difficulty. It is noted that 32 conditions were established with good lubricant and contaminated lubricant by inducing solid particle contamination with different sizes and concentrations. Sensor signatures are investigated using RMS mean plots to gain additional insight into the lubricant conditions.

To understand the variation in the sensor signal due to the increase in the size of the solid particles, mean RMS values are plotted against particle size (P1, P2, P3, P4, and P5). Sensor signature (RMS) correlation with solid particle concentration for different particle sizes and speed of operation are shown in Fig. 7. Plots are made separately for solid particle concentration levels C1, C2, and C3 by operating the bearing under low speed (LS) and high speed (HS). It is observed that considering sound, vibration, and AE signatures, the RMS amplitude increases with the increase in concentration level of solid particle contamination in lubricant for almost all cases. RMS amplitude of high-speed conditions is higher compared to low-speed conditions for almost all particle sizes. An increase in RMS amplitude is also noticed when there is an increase in particle size for sound and vibration sensor signatures. In the case of AE signature, the amplitude of AE is less when the particle of size P1 and increases slightly when the particle size increases. The AE amplitude is reduced with the higher particle size of P5. AE emissions are due to high-frequency excitations due to the interaction of

TABLE 2. Lubricant conditions.

Ex No.	Lubricant Condition (LC)	Parameters	Speed (RPM) LS/HS	Ex No.	Lubricant Condition	Parameters	Speed (RPM) LS/HS
E1	LC1	Fresh Lubricant	800	E9	LC17	P3C2	800
	LC2		1300		LC18		1300
E2	LC3	P1C1	800	E10	LC19	P3C3	800
	LC4		1300		LC20		1300
E3	LC5	P1C2	800	E11	LC21	P4C1	800
	LC6		1300		LC22		1300
E4	LC7	P1C3	800	E12	LC23	P4C2	800
	LC8		1300		LC24		1300
E5	LC9	P2C1	800	E13	LC25	P4C3	800
	LC10		1300		LC26		1300
E6	LC11	P2C2	800	E14	LC27	P5C1	800
	LC12		1300		LC28		1300
E7	LC13	P2C3	800	E15	LC29	P5C2	800
	LC14		1300		LC30		1300
E8	LC15	P3C1	800	E16	LC31	P5C3	800
	LC16		1300		LC32		1300

Note :
P1-Fe Particle Size 5 µm; P2 – Fe Particle size 10 µm; P3 – Fe Particle size 37 µm; P4 – Fe Particle size 74 µm; P5-Fe Particle size 100 µm ; (SiC particle of size 10 µm is added to all conditions); C1-Soild particle concentration (5%); C2-Soild particle concentration (10%); C1-Soild particle concentration (15%)

solid particles with the bearing surface. Since AE is recorded by the sensors between 150 and 400 KHz in frequency, external disturbances like vibration and sound will not be impacted.

It is observed that conditions, viz., the speed of bearing operation, particle size, and its concentration in lubricants, have unique signature patterns. Having the time domain signature and simple statistics will not be adequate to assess the lubricant's condition in real-time; additional analysis of the signature is needed. Time domain signature and simple RMS statistics provide an indication that there is an apparent variation in the signature pattern and its statistics pertaining to fresh lubricant and lubricant contaminated with solid particles. In this study, ML models are developed to predict the lubricant conditions with five different particle sizes, three concentration levels, and two different speeds of operation of SRB using statical features extracted from the time domain signals of sound, vibration, and AE.

C. FEATURE EXTRACTION AND SELECTION

A feature in ML and pattern recognition is a quantifiable attribute of a sensor signature. The effectiveness of pattern recognition, classification, and regression tasks depends critically on the extraction and selection of independent, discriminating, and informative features. In this work, statistical characteristics are taken from the vibration, sound, and AE sensor signatures of various lubricant conditions. To train ML algorithms features with important information about the process conditions are chosen. Trained ML models are used to predict the lubricant conditions. The statistical features are extracted by further processing of the time domain data that was collected from the sensors of 32 lubricant conditions. From the sound and vibration features, a total of eleven features are extracted: a)variance, b)kurtosis, c)skewness, d)mean, e)sum, f)median, g)minimum, h)maximum, i)mode, j)standard-deviation, and k)RMS. Thirteen characteristic features are extracted from the signature of the AE sensor: a)rise, b)count, c)amplitude, d)amplitude-frequency, e)RMS, f)ASL, g)PCNTS, h)rise-frequency, i)I-frequency, j)signal-strength, k)absolute energy, l)C-frequency, and m)P-frequency.

Feature selection improves the performance of ML models by selecting the most significant features and eliminating redundant and irrelevant features. Feature selection also reduces the computational complexity of ML models since training and testing times are reduced. A Relief algorithm proposed by Kira and Rendell [61] has been implemented in this study to select the best features for training and testing the ML models. Feature score is computed for each feature, ranking is done, and top-scoring features are selected for building the ML model. From the sound signal, eight features, namely mean, sum, maximum, skewness, kurtosis,

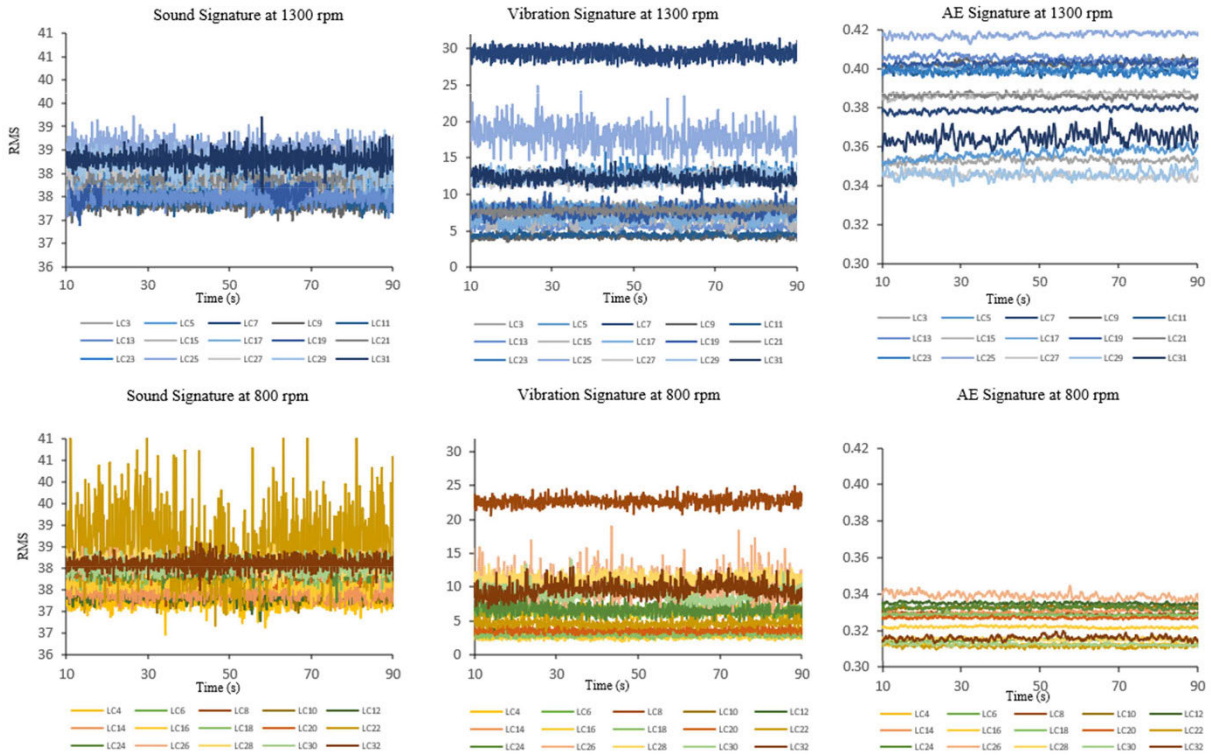

FIGURE 6. Sensor signature patterns of Lubricant Conditions (LC3 to LC32).
Note: Lubricant Conditions (LC): LC3, LC5, LC7, LC9, LC11, LC13, LC15, LC17, LC19, LC21, LC23, LC25, LC27, LC29, and LC31 – SRB operated with 1300 rpm with varied solid particle size (P1, P2, P3 & P4) and concentration (C1, C2, and C3) in lubricant.

standard deviation, variance, and RMS features, are selected. Features viz., mean minimum, maximum, standard deviation, kurtosis, skewness, and RMS were selected from the vibration features. From the AE signature, six features, viz. count, RMS, signal strength, absolute energy, P-frequency, and C-frequency, are selected. Features extracted from the raw signatures are used to train the ML algorithms to predict the lubricant conditions. CART, bagged tree, and SVM methods are used to build the statistical models using the features of sound, vibration, and AE.

D. SENSOR SIGNATURE FEATURE FUSION

In this study, multiple sensors, namely microphones, accelerometers, and piezoelectric sensors, are used to capture the sound, vibration, and AE signatures of lubricant conditions. It is observed from the literature that the reliability of ML models can be improved by training the ML models using fused features of multiple sensor signatures. The basic idea of fusion methodology is to use the strength of each sensor and to build a robust and reliable model [62]. There are different approaches for sensor fusion, namely a) data level fusion, b) feature level fusion, c) decision level fusion, and d) hierarchical sensor level fusion. In this study, we have adopted a feature-level future approach to build the ML model. The methodology is shown in Fig. 8. Fused feature sets of sound, vibration, and AE are used to train the CART, ensemble (bagged tree), and SVM algorithms separately, and their performances are compared.

V. MACHINE LEARNING MODELS FOR LUBRICANT CONDITION PREDICTION

Sensor signature features of 32 lubricant conditions are used to train ML algorithms. In this study, the lubricant conditions are predicted using a)CART, b)Bagged-Tree, and c)SVM algorithms. For every lubricant condition, 1024 data points are used to train the ML algorithms. A 10-fold cross-validation is used in this study to train and test the ML models with the objective of reducing bias and variance. To comprehend the prediction capacity of the classifiers taken into consideration in this study, performance measures such as a) classification-accuracy, b)sensitivity, c)specificity, d)precision, e)recall, f)Kappa, g) MCC and f)F-Measure are computed.

A. DECISION TREE

Decision Tree algorithms are ML algorithms for making predictions. Decision Trees supervised learning models and tree structures are established to make predictions [63]. Different decision tree algorithms used for classifying the data include ID3, C4,5, and CART. CART is one of the approaches used to build the decision trees for prediction. CART algorithms are used for solving classification and regression problems. In the CART algorithm, the training data, i.e., feature data points of the sensor's signatures, are fed into the root node, and the node is split into two child nodes, considering the best attribute and threshold value. The child nodes further split

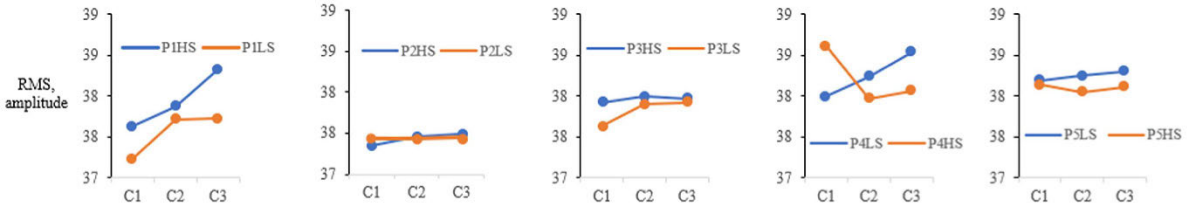

Fig. (a) Sound signature – RMS amplitude variation due to solid particle concentration (C1,C2 & C3) and particle size (P1,P2,P3,P4 & P5) under Low Speed (LS) & High Speed (HS) bearing operating conditions

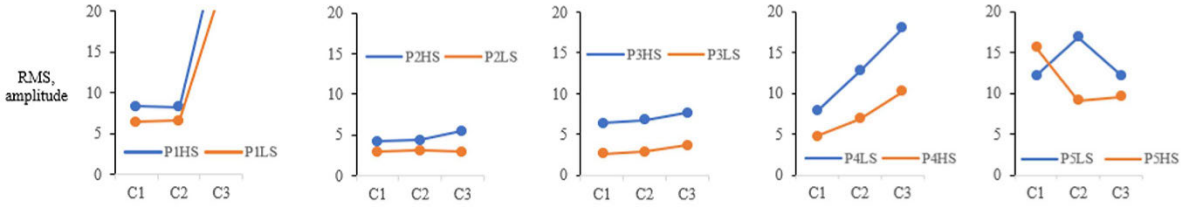

Fig. (b) Vibration signature – RMS amplitude variation due to solid particle concentration (C1,C2 & C3) and particle size (P1,P2,P3,P4 & P5) under Low Speed (LS) & High Speed (HS) bearing operating conditions

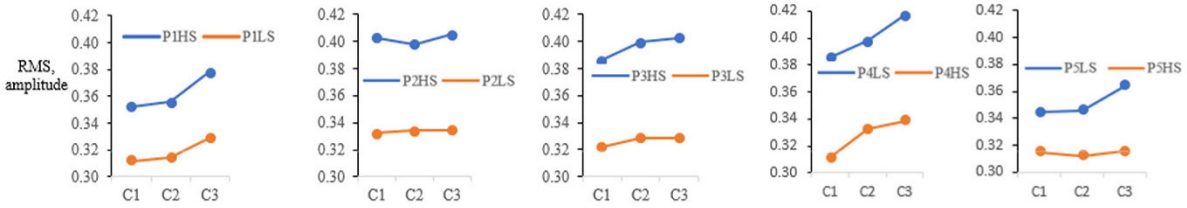

Fig. (c) AE signature – RMS amplitude variation due to solid particle concentration (C1,C2 & C3) and particle size (P1,P2,P3,P4 & P5) under Low Speed (LS) S & High Speed (HS) bearing operating conditions

FIGURE 7. **Sensor signature (RMS) correlation with solid particle concentration for different particle sizes and speed of operation. Note: Lubricant Conditions (LC): LC4, LC6, LC8, LC10, LC12, LC14, LC16, LC18, LC20, LC22, LC24, LC26, LC28, LC30, and LC32 – SRB operated with 800 rpm with varied solid particle size (P1, P2, P3 & P4) and concentration (C1, C2, and C3) in lubricant.**

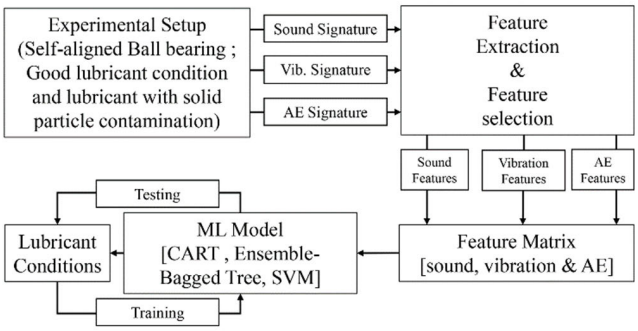

FIGURE 8. **Feature-level fusion methodology.**

again based on the attribute and threshold until the last pure subset, called the leaf node, is found on the growing tree [64]. Three criteria are used in this study to split the nodes, including a)maximum-deviance, b)towing, and c)Gini. With a value ranging from 0 to 1, the Gini Index divides the node according to the likelihood that a randomly selected variable will be classified incorrectly. The Gini-index or Gini- impurity for a node 't' is computed using equation (1). The Gini index value of '0' indicates all the data points belong to only one class; a value of '1' indicates the input data is randomly distributed across all the conditions.

$$Gini\ Impurity_t = 1 - \sum_{i=1}^{n} (P_i)^2 \tag{1}$$

where 'Pi' is the probability of an instance belonging to a particular condition and 'n' is the number of conditions.

For the 'left (l)' and 'right (r)' descendant nodes, the Gini impurity is computed using equations (2) and (3).

$$Gini\ Impurity_l = 1 - \sum_{i=1}^{n} \left(|P_{i|l}\right)^2 \tag{2}$$

$$Gini\ Impurity_r = 1 - \sum_{i=1}^{n} \left(|P_{i|r}\right)^2 \tag{3}$$

where, $P_{n|l}$ and $P_{n|r}$ are the proportions of n^{th} class on the 'left' and 'right' descendent node, respectively.

The Gini criterion for goodness of split (GOF) used for node split is given in equation (4).

$$GOF_{Gini} = Gini\ Impurity_t - P_l Gini\ Impurity_l - P_r Gini\ Impurity_r \tag{4}$$

where 'P_l' and 'P_r' are the percentages of instances on 'left' and 'right' descendent nodes, respectively.

Towing rule has been implemented in CART to measure the change in the probability that a class is in the

left-descendant node rather than the right-descendant node. The towing criterion computes the best splitting value, which maximizes the function given in equation (5).

$$Towing\ function = \frac{P_l P_r}{4}\left[\sum_{i=1}^{n} \left|P_{i|l} - P_{i|r}\right|\right]^2 \quad (5)$$

where 'P_l' and 'P_r' are the percentages of instances on 'left' and 'right' descendent nodes, respectively. The '$P_l P_r$' is implemented for favoring even split.

Maximum Deviance Reduction (MDR) criteria is another essential parameter used to define the goodness of split, indicating how well the tree is reproducing the conditional distribution of the response variable for each possible profile. It measures the node impurity, indicating the deviations of the predicted value by the model from the target. The deviance can be expressed as shown in equation (6).

$$Deviance\ measure = -\sum P(i) \log 2P(i) \quad (6)$$

In this study, the CART algorithm is implemented to predict the lubricant conditions in an SRB. Three criteria, namely Gini, Towing, and MDR criteria, are used as split criteria at nodes. Classification accuracies of CART using different split criteria are compared.

B. ENSEMBLE METHODS

The common issues with CART algorithms include overfitting, high variance, and low bias. When the tree accounts for a lot of the noise in the data and produces an erroneous conclusion, it is said to be overfit. A slight variation in the data can produce a very significant variation in the prediction, which will affect the outcome's stability. The bias of a complicated decision tree is often low. The model finds it highly challenging to include any fresh data as a result.

Meta models, known as ensemble methods, integrate multiple machine-learning techniques into a single predictive model in order to reduce variance (bagging), boost bias (boosting), or enhance predictions (stacking). One approach in the ensemble makes use of the sequential method, capitalizing on the mutual dependence of the base learners. In the parallel ensemble approach, the overall classifier performance can be boosted by weighing previously mislabelled examples with higher weight. The primary motivation for parallel methods is to take advantage of the independence between base learners. The ensembles improve the accuracy of prediction by combining many ML algorithms. In this study, the bagged decision tree approach is used to predict the lubricant solid particle contamination in SRB. Bagged trees are a well-known technique for enhancing the prediction power of a decision tree, which accesses the insight of many decision-tree models [65]. The bagging is a two-step process, viz. a) Bootstrapping and Training and b) Aggregation. The bagging process used in this study for predicting the solid particle lubricant condition in an SRB is shown in Fig. 9.

Step 1: Bootstrap and Training

a) Drawing a sample from the original training dataset with a replacement

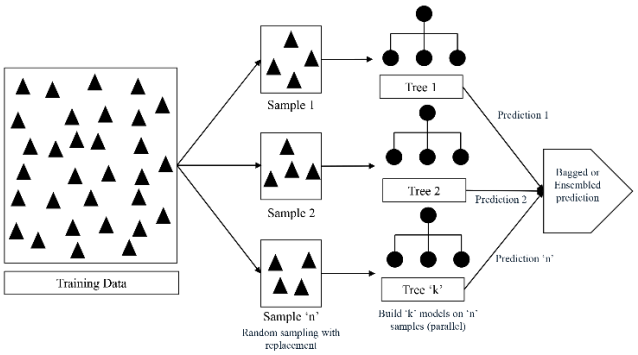

FIGURE 9. Bagging process.

b) Train the decision tree models using the sampled dataset.

c) Repeat Steps 1 and 2 to the set value.

Step 2: Aggregate

a) Generate predictions from each of the trees separately.

b) Aggregate the predictions together to get the final prediction.

C. SUPPORT VECTOR MACHINE

Supervised algorithms such as Support Vector Machine (SVM) are employed to solve classification and regression problems [66]. SVM performs data transformation based on the selected kernel function. Primarily, SVM maximizes the separation boundaries between the classes. The separation of classes is based on kernel functions, namely a) linear, b) polynomial, c) Gaussian, d) Radian Basic Function, and e) Sigmoid. SVM supports binary and multi-class classification. This study looks at a multi-class classification problem with the goal of categorizing 32 lubricant conditions using a cubic kernel function. For multi-class classification, there are two approaches, namely a) the one-to-one approach and b) the one-to-rest approach. The multi-class problem is split up into several binary classification problems in a 'one-to-one' method. For every pair of classes, a binary classifier is employed. The no. of SVMs used in the one-to-one approach is given in equation (7). In the one-to-rest approach, one class is compared with the rest of the class data, and 'n' no. of SVMs will be used for prediction. All SVMs will forecast whether a given condition or class belongs to one of the 'n' classes.

$$\text{No. of SVMs} = \frac{n(n-1)}{2} \quad (7)$$

where 'n' is the no. of conditions.

The 'one-to-rest' approach is used in this study to classify lubricant condition data extracted from the sensors into 32 classes. It should be mentioned that the 'one-to-rest' approach has less computational complexity than the 'one-to-one' approach. The SVM method uses hyperplanes to divide the data into its respective classes. If the data set is non-linear, it is difficult for the algorithm to classify the data using a linear hyperplane. The data generated using the sound, vibration, and AE are non-stationary and non-linear. The

important hyperparameter of SVM is kernels. Kernel tricking is carried out in SVM to separate the non-linear data into linearly separable. There are various kernel methods used in SVM, including linear, polynomial, sigmoidal, and radial basis functions.

The linear kernel for two vectors x and y representing data sets 'A' and 'B' can be expressed as a dot product of vectors x and y. The linear kernel is shown in equation (8). Liner kernel is one of the fastest implementations in SVM.

$$K(x, y) = \left(x^T y\right) \tag{8}$$

The polynomial kernel is defined as shown in equation (9).

$$K(x, y) = \left(\gamma . x^T y + c\right)^d \tag{9}$$

where γ and c are free parameters; $\gamma > 0$ and $c \geq 0$; d is the degree of the polynomial.

Gaussian kernel is an example of a Radial Basis Function (RBF). The RBF kernel is defined as shown in equation (10). One of the most critical parameters affecting SVM performance is 'σ'. The euclidean-distance between 2 feature vectors is defined as $\|x - x'\|$.

$$K(x, y) = e^{\left(-\frac{\|x-y\|^2}{2\sigma^2}\right)} \tag{10}$$

An equivalent definition using the parameter 'σ',
The parameter 'γ' is defined as $1/2\sigma^2$
The RBF kernel can be expressed as shown in equation (11).

$$K(x, y) = e^{(-\gamma \|x-y\|^2)} \tag{11}$$

The sigmoidal kernel is like the sigmoidal function used in logistic regression, and the definition is shown in equation (12).

$$K(x, y) = tanh\left(\gamma . x^T y + c\right) \tag{12}$$

While implementing SVM for the prediction type of problems, the hyperparameters need to be appropriately tuned to improve their classification ability. To classify the lubricant solid particle contamination conditions in an SRB, we have implemented an SVM algorithm with a cubic kernel function.

D. PERFORMANCE MEASURES

ML models are evaluated using various performance measures. Some of the metrics used for evaluation include accuracy, confusion matrix, receiver operating characteristics, precision, recall, F1 score, kappa statistics, and Matthew's correlation coefficient [67]. Researchers rarely use any one of the matrices separately to access the model. It is suggested to assess the no. of matrices and weigh up the trade-offs to decide on the prediction ability of models.

Confusion matrix is another crucial metric to access the model in which way its prediction ability is poor. These metrics, namely true-positive, false-positive, true-negative, and false-negative, are used to study the prediction ability of models. The true-positive value indicates that no. of the positive observed instances is correctly classified as positive instances by the model. The number of positive observed instances that are incorrectly classified as positive is termed as false-positive instances. In similar lines, true-negative and false-negative instances are defined. The accuracy value of the model is computed as shown in equation (13).

$$Accuracy = \frac{T_P + T_N}{T_P + F_P + T_N + F_N} \tag{13}$$

Receiver order characteristics curves of a model plot the accuracy of models, and it is best suited for assessing the model without an imbalance of data. To arrive at the model performance, the area under the curve is computed by plotting the false-positive rate vs true-positive rate. Precision is a measure to assess how well the ML model is correctly predicting the positive classes. Precision is computed using $T_P and T_N$ Instances as given in equation (14).

$$Precision = \frac{T_P}{T_P + T_N} \tag{14}$$

Recall or sensitivity of the model indicates the ability of the model to predict all the positive observations of the dataset. Recall is computed as shown in equation (15). The percentage of fault events that the classifier correctly detects is referred to as specificity and is calculated using equation (16).

The F_1 score is the harmonic mean of 'recall' and 'precision'. The F_1 score takes a value between '0' and '1'. A model with a value of '1' indicates that the models predict with perfect 'precision' and 'recall'. The $F1$ score is computed using the formula as shown in Equation (17).

$$Recall\ or\ Sensitivity = \frac{T_P}{T_P + F_N} \tag{15}$$

$$Specificity = \frac{T_N}{T_N + F_P} \tag{16}$$

$$F_1 Score = 2 \times \left[\frac{Precision \times Recall}{Precision + Recall}\right] \tag{17}$$

Kappa statistics compares the observed and expected accuracy. The imbalance in the dataset may be overcome by using the kappa statistics. It computes the kappa value based on no. of instances in each class. Based on the frequency of each class, the observations are taken at random. The kappa statistics are computed using equation (18). Kappa statistics return a value maximum of '1'. The model is nearly perfectly in agreement when the kappa value falls between 0.81 and 1.0. The kappa value between 0.61 and 0.80 shows a high degree of agreement. A moderate agreement can be observed for a kappa value between 0.41-0.60. A kappa statistic below '0.2' has poor or no agreement.

$$Kappa\ value = \left[\frac{Obserbed\ accuracy - Expected\ Accuracy}{1 - Expected\ Accuracy}\right] \tag{18}$$

Matthews Correlation Coefficient (MCC) is another measure to evaluate the ML models. This measure produces

a score in the interval [+1, −1]. The value of '−1' indicates the model as a perfect mis-classifier and '+1' will be a perfect classifier. The prediction receives a high score from the MCC only if it performs well across all four categories, viz. $T_P, F_N, T_N,$ *and* F_P. MCC is computed using the equation (19).

$$MCC = \frac{T_P.T_N - F_P.F_N}{\sqrt{(T_P + F_P)\,.\,(T_P + F_N)\,.\,(T_N + F_P)\,.\,(T_N + F_N)}} \tag{19}$$

The performance of the classifiers taken into consideration in this study has been evaluated using all the metrics as mentioned earlier.

VI. RESULTS AND DISCUSSIONS

A. PERFORMANCE OF ML MODELS TRAINED SEPARATELY WITH SOUND, VIBRATION, AND AE SIGNATURE FEATURES

The performance of ML algorithms trained and tested separately with sound, vibration, and AE signature features are shown in Table 3, Table 4, and Table 5, respectively. In the CART algorithm, three split criteria, namely, Gini, Towing, and MDR criteria are used to study the performance of the CART algorithm. The maximum no. of splits considered is 100. Along with the CART algorithm, Bagged Tree and SVM trained with cubic kernel function are used in this study. For the training bagged tree, the number of splits considered is 32767, and the number of base learners utilized is 40. In a multi-class SVM model, the box constraint level has been chosen as one. The data associated with each test case is categorized using the ''One-to-Rest'' method. The ML algorithms are trained and tested using the following sound and vibration features: a)mean, b)median, c)mode, d)sum, e)minimum, f)maximum, g)skewness, h)kurtosis, i)standard-deviation, j)variance, and k)RMS features. AE features, namely a)rise, b)count, c)RMS, d)ASL, e)PCNTS, f)R-FRQ, g)I-FRQ, h)signal-strength, i)absolute-energy, and j)C-Frequency are used to train and test the ML models. The ML algorithm's prediction ability for the lubrication conditions is assessed using performance measures, including recall, F-measure, sensitivity, specificity, Kappa, MCC, and accuracy.

Based on the findings in Table 3, the ML models trained solely on sound signature features exhibited a modest ability to predict the lubricant condition in SRB with an accuracy of around 61 - 65%. The SVM and Bagged tree models were observed to have marginally higher accuracies compared to the CART models. The Kappa values suggested a substantial agreement between the predicted and actual lubricant conditions. The MCC, however, indicated only a moderate correlation between the predicted and actual lubricant conditions, with the SVM model achieving the highest MCC of just 0.52. The sensitivity values suggest a reasonably high capability to correctly identify true instances of the presence of solid particle contamination. Conversely, the models exhibited only a moderate ability to correctly identify true negative instances, i.e., the absence of solid particle contamination.

TABLE 3. Performance Of Ml algorithms trained using sound signature features.

Algorithm / Measure	CART Algorithm			Bagged Tree	C-SVM
	Gini	Towing	MDR		
Accuracy	0.62	0.62	0.61	0.65	0.65
Mis-classification Rate	0.38	0.38	0.39	0.35	0.35
Sensitivity	0.87	0.88	0.85	0.85	0.87
Specificity	0.61	0.61	0.61	0.64	0.64
Precision	0.69	0.69	0.68	0.70	0.70
F-Measure	0.77	0.78	0.76	0.77	0.78
Kappa	0.74	0.75	0.73	0.75	0.75
MCC	0.50	0.51	0.47	0.51	0.52

The precision, ranging between 0.68 and 0.70, suggests only a moderate ability to correctly predict the presence of solid particle contamination from among the positive classifications. All models exhibited similar levels of F-Measure between 0.76 and 0.78, indicating a similar balance between precision and recall. It is noted that the split criteria did not significantly influence the prediction ability of the CART models, as evidenced by their comparable performance. The 'Towing' criteria provided only a slight performance improvement while the 'MDR' criteria provided slightly worse results than the rest. The SVM model was observed to be slightly better than the Bagged Tree model in terms of sensitivity, F-measure, and MCC.

TABLE 4. Performance Of Ml algorithms trained using vibration signature features.

Algorithm / Measure	CART Algorithm			Bagged Tree	C-SVM
	Gini	Towing	MDR		
Accuracy	0.58	0.61	0.61	0.65	0.64
Mis-classification Rate	0.42	0.39	0.39	0.35	0.36
Sensitivity	0.91	0.92	0.91	0.94	0.93
Specificity	0.57	0.60	0.60	0.64	0.63
Precision	0.68	0.70	0.69	0.72	0.71
Recall	0.91	0.92	0.91	0.94	0.93
F-Measure	0.78	0.79	0.79	0.82	0.81
Kappa Statistics	0.74	0.76	0.76	0.79	0.78
MCC	0.51	0.55	0.54	0.61	0.58

Similar to the previous discussion on sound signature-based models, the ML models trained solely on vibration signature features also exhibited a modest ability to predict the lubricant condition, as indicated by the results in Table 4. The Bagged Tree model was observed to provide the highest accuracy of 65%, with the SVM model performing only slightly worse at 64%. The CART models performed worse with 58-61% accuracy. The split criteria once again

had an insignificant influence on the performance of the CART models, with the 'Towing' and 'MDR' spilt criterion providing slightly better accuracy than 'Gini'. The Kappa also indicated substantial agreement between the predicted and actual lubricant conditions, with the Bagged Tree model exhibiting the highest Kappa of 0.79. The MCC indicated that the models exhibited moderate performance, with the Bagged Tree model achieving the highest MCC of 0.61. The models were observed to have a high capability to correctly identify true instances of the presence of solid particle contamination, as indicated by their high sensitivity, with the Bagged Tree model demonstrating the highest sensitivity of 0.94. However, similar to the case with the sound signature-based models, the ability of the models to correctly identify true negative instances was observed to be moderate, as indicated by their specificities. The models exhibited a moderate ability to correctly predict the presence of solid particle contamination from among the positive classifications, with a precision between 0.68 and 0.72. The Bagged Tree model had the highest F-Measure of 0.82, indicating a better balance between precision and sensitivity compared to the other models.

Overall, when trained solely on sound signature features, the SVM and Bagged Tree models generally outperform the CART models by a small margin. Meanwhile, when trained solely on vibration signature features, the Bagged Tree model outperformed all other models across all the performance measures considered. The ML models trained solely on vibration signature or sound signature features exhibited the highest classification accuracy of around 65%. It is observed that the models trained on vibration signature features generally performed relatively better than those trained on sound signature features across most performance measures such as sensitivity, precision, F-Measure, Kappa, and MCC. However, the overall accuracy and performance of all the models were observed to be relatively modest, suggesting that sound signatures or vibration signatures alone may be insufficient for accurate prediction of lubricant conditions.

TABLE 5. Performance Of Ml algorithms trained using AE signature features.

Algorithm / Measure	CART Algorithm			Bagged Tree	C-SVM
	Gini	Towing	MDR		
Accuracy	0.90	0.90	0.90	0.94	0.93
Mis-classification Rate	0.10	0.10	0.10	0.06	0.07
Sensitivity	0.99	1.00	1.00	1.00	1.00
Specificity	0.89	0.90	0.90	0.94	0.93
Precision	0.90	0.90	0.91	0.94	0.94
F-Measure	0.95	0.95	0.95	0.97	0.97
Kappa Statistics	0.94	0.95	0.95	0.97	0.97
MCC	0.89	0.89	0.90	0.94	0.93

The performance measures of the ML models trained using the AE features are shown in Table 5. The results indicate that, in comparison to models developed using sound and vibration features, models developed using AE features are better at predicting the solid particle lubricant contamination conditions in SRB. In particular, the bagged tree ensemble and SVM models exhibit very good performance across all metrics considered, with accuracy above 93%, near-perfect sensitivity, high specificity, precision, F-Measure, and MCC, and very high Kappa. The near-perfect sensitivity indicates that the models are highly capable of identifying nearly all instances of solid particle contamination. Moreover, the high precision and specificity further emphasize their reliability in correctly identifying lubricant conditions and minimizing false positives. The high F-Measure demonstrates that the models exhibit a good balance between precision and recall. The Kappa Statistics indicate an almost perfect agreement between the predicted and actual lubricant conditions, and the MCC values also indicate a very high performance across all categories, considering true positives, false negatives, true negatives, and false positives. Once again, the split criteria did not significantly influence the performance of the CART models.

The Bagged Tree and SVM models outperformed the CART models regardless of the signature features on which they were trained. This may be attributed to the capability of these models to handle noise and represent the complex non-linear relationships between the features more effectively. The Bagged Tree model, employing the ensemble method, combines the predictions of multiple base learners, which reduce variance and overfitting to improve the overall performance of the model. Meanwhile, the SVM model maps the features into a higher-dimensional space using the cubic kernel function to determine the optimal hyperplanes while also reducing overfitting, resulting in better generalization.

The superior performance of the models trained using the AE signature features compared to the sound and vibration-based models may be attributed to the fundamental differences in the frequency ranges and sensitivity of the sensors. The interaction of solid contaminant particles with the bearing surfaces generates high-frequency acoustic waves that are effectively captured by the AE sensor, as evident from the unique AE signature patterns observed in Fig. 4 for different lubricant conditions. Particularly, the AE sensors capture high-frequency acoustic emission signatures in the range of 150-400 kHz, which are more sensitive to changes in lubricant conditions caused by solid particle contamination. Furthermore, AE sensors amplify the high-frequency AE signals, which may be attenuated or masked by noise in lower frequency ranges. In contrast, sound and vibration sensors, operating at lower frequencies, may be inadequate in detecting subtle changes in lubricant conditions. The ML models built using AE sensors features effectively capture a)variations in particle size, b)solid particle concentration,

TABLE 6. Comparative performance of Ml algorithms trained with sensor signature features separately and combinedly using feature level fusion method.

Algorithm / Measure	Sound	Vibration	AE	Fused Model				
	C-SVM[@]	Bagged Tree[#]	Bagged Tree[$]	CART Algorithm			Bagged Tree	C-SVM
				Gini	Towing	MDR		
Accuracy	0.65	0.65	0.94	0.97	0.97	0.97	0.99	0.98
Misclassification Rate	0.35	0.35	0.06	0.03	0.03	0.03	0.01	0.02
Sensitivity	0.87	0.94	1.00	1.00	1.00	1.00	1.00	1.00
Specificity	0.64	0.64	0.94	0.97	0.97	0.97	0.99	0.98
Precision	0.70	0.72	0.94	0.97	0.97	0.97	0.99	0.98
F-Measure	0.78	0.94	0.97	0.98	0.98	0.98	0.99	0.99
Kappa Statistics	0.75	0.82	0.97	0.98	0.98	0.98	0.99	0.99
MCC	0.52	0.79	0.94	0.97	0.96	0.97	0.99	0.98

Note: @ Best performing ML model (C-SVM) developed using Sound signature features; # Best performing ML model (Bagged Tree Ensemble) developed using Vibration signature features; $ Best performing ML model (Bagged Tree Ensemble) developed using AE signature features

and c)speed of operation of bearing and predict the lubricant conditions with reasonable accuracy.

B. PERFORMANCE OF ML ALGORITHMS TRAINED WITH FUSED FEATURES OF SOUND, VIBRATION, AND AE SIGNATURES

ML models have been trained with the fusion of all sensor signal features at the feature level in an attempt to increase their prediction accuracy and reliability. The approach involved combining selected features from the sound, AE, and vibration sensor signatures into a shared database. A total of 34 features, comprising 11 features each from sound and vibration and 12 from AE, are utilized to train the ML models for predicting 32 different lubricant conditions. The study employed CART, Bagged Tree, and Cubic Kernel SVM algorithms, which were trained and tested using 10-fold cross-validation. The performances of the ML models were evaluated using the metrics employed prior, viz., accuracy, sensitivity, specificity, precision, recall, F-Measure, kappa, and MCC. The feature data points were extracted from 100 seconds of operation for each condition, resulting in a total of 892,160 data points for training the ML algorithms.

The performance of the ML algorithms using the fused feature data comprising all sensor signature features is presented in Table 6. The best-performing models trained separately on vibration, sound, and AE features are compared with the models trained using the feature-level fusion approach. The results demonstrate that the fusion models using Bagged Tree, SVM, and CART algorithms outperform the models trained separately on individual sensor signature features by a wide margin. Notably, the Bagged Tree, SVM, and CART models achieved high classification accuracies of 99%, 98%, and 97%, respectively, in predicting lubricant conditions in SRB. The split criteria had no significant influence on the performance of the CART models. The perfect sensitivity (100%) and near-perfect specificity (above 97%) of the models trained using the feature-level fusion approach demonstrate their outstanding capability to correctly identify all instances of solid particle contamination while minimizing false positives. The high precision (above 97%) and F-Measure values (above 98%) further indicate the reliability of the models in classifying lubricant conditions, with a good balance between precision and sensitivity. The Kappa values also indicate near-perfect agreement between actual and predicted lubricant conditions. The high MCC reinforces the reliable performance of the models trained using the feature-level fusion approach.

The Bagged Tree and SVM models trained using the fusion approach are observed to provide very high performance across all evaluation measures considered. The Bagged Tree model is also found to outperform the SVM model by a very slight margin. The findings indicate that the fusion approach can significantly improve the performance of the various ML algorithms examined in the study. The high performance of the ML models trained using the feature-level fusion approach may be attributed to the complementary nature of the data provided by the different sensor signatures. By combining the sound, vibration, and AE signature features into a unified feature vector, the models can effectively exploit the strengths of each sensor modality, thereby obtaining a more comprehensive representation of the lubricant condition. The fusion approach captures the unique characteristics of each sensor modality, allowing the ML models to discriminate between the different classes more easily.

The Confusion Matrix (CM) of the best-performing Bagged Tree ensemble model is shown in Table 7. The CM provides an overview of the classification results of the ML model, displaying the prediction counts of true-positive, true-negative, false-positive, and false-negative values. The diagonal values indicate the number of instances that were correctly classified. Out of 26,240 features, the Bagged Tree model correctly classified 25,882 features corresponding to the lubricant condition. Lubricant conditions LC1 and LC2 represent fresh lubricants without any solid particle contamination,

TABLE 7. Confusion matrix of best performing algorithm – bagged tree model trained with sound, vibration, and AE signature features (feature level fusion model).

ACTUAL \ LC	1	2	3	4	5	6	7	8	9	10	11	12	13	14	15	16	17	18	19	20	21	22	23	24	25	26	27	28	29	30	31	32
32	0	0	0	0	0	0	0	0	0	0	0	0	0	0	0	0	0	0	0	0	0	0	0	0	0	0	0	8	0	11	2	**799**
31	0	0	0	0	0	0	0	0	0	0	0	0	0	0	0	0	0	0	0	0	0	0	0	0	0	0	0	0	0	0	**818**	2
30	0	0	0	0	0	0	0	0	0	0	0	0	0	0	0	0	0	0	0	0	0	0	0	0	0	0	0	0	0	**805**	0	15
29	0	0	0	0	0	0	0	0	0	0	0	0	0	0	0	0	0	0	0	0	0	0	0	0	0	1	53	0	**750**	0	16	0
28	0	0	0	0	0	0	0	0	0	0	0	0	0	0	0	0	0	0	0	0	0	0	0	0	0	0	0	**810**	0	4	0	6
27	0	0	0	0	0	0	0	0	0	0	0	0	0	0	0	0	0	0	0	0	0	0	0	0	0	4	**767**	0	45	4	0	0
26	0	0	0	0	0	0	0	0	0	0	0	0	0	0	0	0	0	0	0	0	0	12	0	1	0	**789**	0	2	0	16	0	0
25	0	0	0	0	0	0	0	0	0	0	0	0	0	0	0	0	0	0	0	0	4	0	0	0	**814**	0	0	2	0	0	0	0
24	0	0	0	0	0	0	0	0	0	0	0	0	0	0	0	0	0	0	0	0	0	1	0	**815**	0	4	0	0	0	0	0	0
23	0	0	0	0	0	0	0	0	0	0	0	0	0	0	0	0	0	0	0	0	14	0	**800**	0	6	0	0	0	0	0	0	0
22	0	0	0	0	0	0	0	0	0	0	0	0	0	0	0	0	0	0	0	0	0	**790**	10	5	0	15	0	0	0	0	0	0
21	0	0	0	0	0	0	0	0	0	0	0	0	0	0	0	0	0	1	0	3	**800**	2	14	0	0	0	0	0	0	0	0	0
20	0	0	0	0	0	0	0	0	0	0	0	0	0	0	0	0	0	6	2	**809**	3	0	0	0	0	0	0	0	0	0	0	0
19	0	0	0	0	0	0	0	0	0	0	0	0	0	0	0	0	0	0	**820**	0	0	0	0	0	0	0	0	0	0	0	0	0
18	0	0	0	0	0	0	0	0	0	0	0	0	0	0	0	0	1	**808**	3	8	0	0	0	0	0	0	0	0	0	0	0	0
17	0	0	0	0	0	0	0	0	0	0	0	0	0	0	0	0	**820**	0	0	0	0	0	0	0	0	0	0	0	0	0	0	0
16	0	0	0	0	0	0	0	0	0	0	0	0	0	1	0	**814**	3	2	0	0	0	0	0	0	0	0	0	0	0	0	0	0
15	0	0	0	0	0	0	0	0	0	0	0	0	0	1	**817**	2	0	0	0	0	0	0	0	0	0	0	0	0	0	0	0	0
14	0	0	0	0	0	0	0	0	0	0	0	0	0	**818**	2	0	0	0	0	0	0	0	0	0	0	0	0	0	0	0	0	0
13	0	0	0	0	0	0	0	0	0	0	3	0	**817**	0	0	0	0	0	0	0	0	0	0	0	0	0	0	0	0	0	0	0
12	0	0	0	0	0	0	0	0	0	4	0	**801**	1	14	0	0	0	0	0	0	0	0	0	0	0	0	0	0	0	0	0	0
11	0	0	0	0	0	0	0	0	0	0	**811**	4	5	0	0	0	0	0	0	0	0	0	0	0	0	0	0	0	0	0	0	0
10	0	0	0	0	0	0	0	0	0	**820**	0	0	0	0	0	0	0	0	0	0	0	0	0	0	0	0	0	0	0	0	0	0
9	0	0	0	0	0	0	0	0	**820**	0	0	0	0	0	0	0	0	0	0	0	0	0	0	0	0	0	0	0	0	0	0	0
8	0	0	0	0	0	0	0	**820**	0	0	0	0	0	0	0	0	0	0	0	0	0	0	0	0	0	0	0	0	0	0	0	0
7	0	0	0	0	0	0	**820**	0	0	0	0	0	0	0	0	0	0	0	0	0	0	0	0	0	0	0	0	0	0	0	0	0
6	0	0	0	1	0	**818**	1	0	0	0	0	0	0	0	0	0	0	0	0	0	0	0	0	0	0	0	0	0	0	0	0	0
5	0	0	3	0	**817**	0	0	0	0	0	0	0	0	0	0	0	0	0	0	0	0	0	0	0	0	0	0	0	0	0	0	0
4	0	0	0	**819**	0	1	0	0	0	0	0	0	0	0	0	0	0	0	0	0	0	0	0	0	0	0	0	0	0	0	0	0
3	0	0	**816**	1	3	0	0	0	0	0	0	0	0	0	0	0	0	0	0	0	0	0	0	0	0	0	0	0	0	0	0	0
2	0	**820**	0	0	0	0	0	0	0	0	0	0	0	0	0	0	0	0	0	0	0	0	0	0	0	0	0	0	0	0	0	0
1	**820**	0	0	0	0	0	0	0	0	0	0	0	0	0	0	0	0	0	0	0	0	0	0	0	0	0	0	0	0	0	0	0

PREDICTED

Note :
Lubricant Conditions (LC); LC:1-2 (Fresh lubricant); LC3-8 (bearing operated with particle size 5µm); LC9-14 (bearing operated with particle size 10µm); LC15-20 (bearing operated with particle size 72µm); LC21- 26 (bearing operated with particle size 74µm); LC7-32 (bearing operated with particle size 100µm)

with the bearing operated at 800 and 1300 rpm, respectively. Under these conditions, no misclassifications are observed, and all features are classified correctly by the model.

Condition LC3-LC8 represents a particle size of 5μm with three different concentrations and bearings operated under two different speed conditions. In these conditions, among 4,920 data features, only 10 data features were misclassified. There were 33 and 31 misclassifications observed under conditions LC9-LC14 and LC15-LC20, respectively, with solid particle sizes of 10μm and 37μm. In conditions LC21-LC26, the bearing operated with solid particle contaminants of size 74μm, and the number of misclassifications observed was 112. In the case of particle size 100μm corresponding to conditions LC27-LC32, 171 instances were misclassified. It is noted that as solid particle contamination increased, the number of misclassifications predicted by the model also increased. This increase was marginal at lower particle sizes but became more apparent at larger particle sizes. It is observed from the CM that most misclassifications occurred between similar lubricant conditions, especially those with larger particle sizes and higher concentrations. This may be attributed to the fact that sensor signals were captured at discrete conditions rather than in a continuous manner, leading to potential overlaps in the feature space between

TABLE 8. Performance of bagged tree model trained with sound, vibration, and AE signature features (feature level fusion model).

Solid Particle contamination size, µm	Prediction ability of ML model (Accuracy, %)					
	Speed of Operation		Concentration, %			Overall
	Low	High	Low	Medium	High	
0	100	100	-	-	-	100
5	99.72	99.88	99.80	99.80	100	99.80
10	99.55	99.23	100	98.29	99.82	99.37
37	99.88	98.82	99.45	99.27	99.33	99.35
74	98.13	97.32	96.95	98.48	97.81	97.72
100	94.96	98.13	96.16	94.76	98.54	96.52

neighboring conditions. The overlapping feature distributions of similar conditions may affect the ability of the model to separate them effectively. The model exhibited very few misclassifications for extreme conditions, such as conditions with fresh lubricant with no contamination or conditions with low particle size and low concentration, indicating the reliability of the model in distinguishing between these distinct classes.

There were only 36 instances where the model misidentified conditions with different particle sizes, and these misclassifications were only observed between neighboring particle sizes. The majority of these misclassifications were between the lubricant conditions with larger particle sizes of 74μm and 100μm, with 20 instances of conditions with 74μm particles being mistaken for conditions with 100μm particle contaminants. Meanwhile, five instances of conditions with 100μm particles were mistaken for conditions with 74μm particles. Additionally, there were even fewer misclassifications involving the particle size of 37μm, where it was confused with 74μm and 10μm particle sizes. Notably, no misclassifications were observed between the conditions with fresh lubricant and those with particle contaminants of sizes 5μm and 10μm. The total misclassifications between lubricant conditions with different sizes of solid particle contamination amount to less than 0.15% of the total classifications. These results indicate that the fused model can effectively distinguish the sensor signature features associated with the varying sizes of particle contamination.

For lubricant conditions with particles of size 5μm, no misclassifications were observed for instances with high concentrations of solid particle contamination, irrespective of operation speed. However, misclassifications were observed when differentiating between the low and medium concentrations. Similarly, no misclassifications were observed at low concentrations for conditions with particles of size 10μm. However, misclassifications were evident at medium and high concentrations of solid particle contaminants. Some misclassifications related to operating speed conditions were present in both 5μm and 10μm scenarios, though marginal. As particle sizes increased to 37μm and above, the model experienced more significant challenges in differentiating solid particle concentrations accurately. The number of misclassifications related to particle concentration progressively increased for larger particle sizes of 74μm and 100μm. Most misclassifications occurred while identifying the correct concentration level rather than the particle size or operating speed. It is evident that while the model is effective at detecting the presence of particle contamination, discriminating between different concentrations becomes more complicated when dealing with lubricant contamination scenarios involving larger particles at low to medium concentrations.

To provide a comprehensive understanding of the predictive capabilities of the developed feature-level fusion model, Table 8 presents a detailed analysis of the model's overall prediction accuracy under various lubricant conditions: a) without any solid particle contamination, b) with varying solid particle sizes and concentrations, and c) with two different bearing operating speeds (low & high). It is observed that the ML model predicted all 32 lubricant conditions with reasonable accuracy (above 96.5%). The model predicted fresh lubricant conditions without solid particle contamination with 100% accuracy, demonstrating its reliability in identifying ideal operating conditions. The classification ability decreased slightly as particle size increased, which may be due to the increased complexity in distinguishing between similar contamination levels at higher concentrations. The model exhibited consistently high accuracy while predicting lubricant conditions with contaminants particle sizes of 37μm and less across low, medium, and high concentrations. However, the accuracy varied much more across the different concentrations for conditions with larger particle sizes (74μm and 100μm), indicating that the concentration of larger particles has a more significant impact on the model's performance. Nonetheless, the overall accuracy of the classification remained above 96.5% even for the most challenging condition with contaminants of particle size 100μm. The results also show that the model had slight difficulties determining the condition of lubricant with contaminant particles of size 100μm while operating at low speed and low to medium concentrations.

In conclusion, the fusion of sound, vibration, and AE signature features using the robust Bagged Tree ensemble algorithm enables reliable classification of lubricant conditions in SRB under various operating scenarios. The model has demonstrated the ability to generalize across diverse conditions, including varying particle sizes, concentrations, and operating speeds.

VII. CONCLUSION

In this present study, statistical models were developed using ML algorithms with the sound, vibration, and AE sensor signature features acquired by operating the bearing under fresh lubricant and lubricant with solid particle contamination. Lubricant contaminant conditions were established by adding Iron and Silicon carbide particles at different sizes and concentrations in a controlled manner. A total of 32 lubricant conditions were established. Sensor signatures were acquired by operating the SRB under two different speed conditions.

RMS statistics derived from the time domain signature of AE exhibit a unique pattern for all 32 lubricant conditions considered in this study. This shows the dominance of AE compared to sound and vibration signatures in differentiating the lubricant conditions. It is also noted that an increase in the size and concentration of solid particles used in lubricant has a significant impact on the RMS signature amplitude. The increase in particle size and concentration results in an increase in the amplitude of the sound, vibration, and AE signatures for almost all conditions. Sensor signature patterns and RMS statistics indicate that sound, vibration, and AE signatures captured the particle contamination conditions in the lubricant effectively.

For predicting the lubricant conditions, ML models are developed using the statistical features extracted from sensor signatures of all 32 lubricant conditions. CART, Bagged tree ensemble, and Support Vector Machines were employed. Feature-level fusion models were developed in this study to improve the prediction ability of ML models. The classification ability of ML models was compared by training the ML models with signature features separately and combined by fusing the sound, vibration, and AE features at the feature level.

Among the ML models developed in this study, models trained with AE signature features outperform models built with vibration and sound signature features. Decision trees built using Gini, Towing, and MDR split criterion, the bagged tree ensemble model, and SVM trained with cubic kernel function predict the lubricant conditions with an accuracy of more than 90%. The interaction of solid particle contaminants with the bearing surface resulted in the generation of AE waves, and are well captured by the AE sensor. AE sensors are sensitive to capture the slight variations in the AE due to changes in particle size, speed of operation, and concentration of solid particles in the lubricant.

Online monitoring needs a robust model to predict the condition of the lubricant. A feature-level fusion methodology adopted in this study improved the prediction ability of the ML models. All models achieved an accuracy of more than 97%. The bagged tree ensemble predicted the lubricant conditions with a maximum accuracy of 99%. CART algorithm and SVM algorithms can detect the lubricant condition with an accuracy of 98% and 97%, respectively.

The proposed approach can be used to develop a real-time lubricant condition monitoring system to adopt condition-based maintenance. When compared to models created using vibration and sound signature features, AE-based ML models prove to be effective in predicting the lubricant conditions, and the fusion model improved the classification ability of all ML models considered in this study.

The experiments for the study were conducted in a controlled laboratory environment, which may not fully reflect the conditions encountered in a real-world industrial environment. The study extracted the sensor signature features using time domain signatures for developing ML models. The data used in the study was collected for a limited duration by artificially introducing solid particle contaminants of different sizes and concentrations. The long-term effects of lubricant contamination due to wear and particle generation may be investigated further. These limitations may be addressed in future studies to improve the reliability and generalization capability of the models. Further ML models can be developed using features extracted from frequency and time-frequency domains for predicting the lubricant contaminant conditions in different types of bearings and lubricants.

REFERENCES

[1] C. Radu, "The most common causes of bearing failure and the importance of bearing lubrication," *RKB Tech. Rev.*, pp. 1–7, Feb. 2010. [Online]. Available: https://pdf.directindustry.com/pdf/rkb-europe/most-common-causes-bearing-failure-importance-bearing-lubrication/27918-138476.html

[2] R. Nilsson, R. S. Dwyer-Joyce, and U. Olofsson, "Abrasive wear of rolling bearings by lubricant borne particles," *Proc. Inst. Mech. Eng., J, J. Eng. Tribol.*, vol. 220, no. 5, pp. 429–439, Aug. 2006, doi: 10.1243/13506501j00205.

[3] R. S. Dwyer-Joyce, "Predicting the abrasive wear of ball bearings by lubricant debris," *Wear*, vols. 233–235, pp. 692–701, Dec. 1999, doi: 10.1016/s0043-1648(99)00184-2.

[4] H. Zhou, X. Huang, G. Wen, Z. Lei, S. Dong, P. Zhang, and X. Chen, "Construction of health indicators for condition monitoring of rotating machinery: A review of the research," *Exp. Syst. Appl.*, vol. 203, Oct. 2022, Art. no. 117297, doi: 10.1016/j.eswa.2022.117297.

[5] R. Bogue, "Sensors for condition monitoring: A review of technologies and applications," *Sensor Rev.*, vol. 33, no. 4, pp. 295–299, Sep. 2013, doi: 10.1108/sr-05-2013-675.

[6] R. S. Dwyer-Joyce, "The effects of lubricant contamination on rolling bearing performance," Ph.D. dissertation, Dept. Mech. Eng., Imperial College London, South Kensington, London SW7 2AZ, UK, 1993.

[7] L. Kahlman and I. M. Hutchings, "Effect of particulate contamination in grease-lubricated hybrid rolling bearings," *Tribol. Trans.*, vol. 42, no. 4, pp. 842–850, Jan. 1999, doi: 10.1080/10402009908982291.

[8] M. M. Khonsari and E. R. Booser, "Effect of contamination on the performance of hydrodynamic bearings," *Proc. Inst. Mech. Eng., J, J. Eng. Tribol.*, vol. 220, no. 5, pp. 419–428, May 2006, doi: 10.1243/13506501j00705.

[9] W. Wang, P. L. Wong, F. He, and G. T. Y. Wan, "Experimental study of the smoothing effect of a ceramic rolling element on a bearing raceway in contaminated lubrication," *Tribol. Lett.*, vol. 28, no. 1, pp. 89–97, Aug. 2007, doi: 10.1007/s11249-007-9251-8.

[10] G. K. Nikas, "A state-of-the-art review on the effects of particulate contamination and related topics in machine-element contacts," *Proc. Inst. Mech. Eng., J, J. Eng. Tribol.*, vol. 224, no. 5, pp. 453–479, May 2010, doi: 10.1243/13506501jet752.

[11] E. Beghini, R. S. Dwyer-Joyce, E. Ioannides, and B. Jacobson, "Elastic/plastic contact and endurance life prediction," *J. Phys. D, Appl. Phys.*, vol. 25, no. 3, pp. 379–383, Mar. 1992, doi: 10.1088/0022-3727/25/3/007.

[12] G. Singotia and A. K. Jain, "Effect of solid contamination in ball bearings—A review," *Int. J. Current Res. Rev.*, vol. 5, no. 12, pp. 119–124, 2013.

[13] C.-L. Lin, M. Pozzebon, K. A. Sokolowski, and P. A. Meehan, "Experimental investigation on rolling contact wear in grease lubricated spherical roller bearings using microcomputed tomography (μCT)," *Wear*, vols. 534–535, Dec. 2023, Art. no. 205121, doi: 10.1016/j.wear.2023.205121.

[14] B. Ding, X. Li, C. Li, Y. Li, and S.-C. Chen, "A survey on the mechanical design for piezo-actuated compliant micro-positioning stages," *Rev. Sci. Instrum.*, vol. 94, no. 10, Oct. 2023, Art. no. 101502, doi: 10.1063/5.0162246.

[15] S. Martin-Del-Campo, S. Schnabel, F. Sandin, and P. Marklund, "Detection of particle contaminants in rolling element bearings with unsupervised acoustic emission feature learning," *Tribol. Int.*, vol. 132, pp. 30–38, Apr. 2019, doi: 10.1016/j.triboint.2018.12.007.

[16] T. Akagaki, M. Nakamura, T. Monzen, and M. Kawabata, "Analysis of the behaviour of rolling bearings in contaminated oil using some condition monitoring techniques," *Proc. Inst. Mech. Eng., J, J. Eng. Tribol.*, vol. 220, no. 5, pp. 447–453, May 2006, doi: 10.1243/13506501j00605.

[17] J. Miettinen and P. Andersson, "Acoustic emission of rolling bearings lubricated with contaminated grease," *Tribol. Int.*, vol. 33, no. 11, pp. 777–787, Nov. 2000, doi: 10.1016/s0301-679x(00)00124-9.

[18] M. Tiboni, C. Remino, R. Bussola, and C. Amici, "A review on vibration-based condition monitoring of rotating machinery," *Appl. Sci.*, vol. 12, no. 3, p. 972, Jan. 2022, doi: 10.3390/app12030972.

[19] M. M. Maru, R. Serrato-Castillo, and L. R. Padovese, "Influence of oil contamination on vibration and wear in ball and roller bearings," *Ind. Lubrication Tribol.*, vol. 59, no. 3, pp. 137–142, May 2007, doi: 10.1108/00368790710746101.

[20] V. Hariharan and P. S. S. Srinivasan, "Condition monitoring studies on ball bearings considering solid contaminants in the lubricant," *Proc. Inst. Mech. Eng., C, J. Mech. Eng. Sci.*, vol. 224, no. 8, pp. 1727–1748, Aug. 2010, doi: 10.1243/09544062jmes1885.

[21] O. L. Mahajan and A. A. Utpat, "Study of effect of solid contaminants in the lubricant on ball bearings vibration," *Int. J. Instrum. Control Autom.*, vol. 1, pp. 28–31, Apr. 2012, doi: 10.47893/ijica.2012.1063.

[22] D. Koulocheris, A. Stathis, T. Costopoulos, and D. Tsantiotis, "Experimental study of the impact of grease particle contaminants on wear and fatigue life of ball bearings," *Eng. Failure Anal.*, vol. 39, pp. 164–180, Apr. 2014, doi: 10.1016/j.engfailanal.2014.01.016.

[23] S. Kulkarni and A. Bewoor, "Vibration based condition assessment of ball bearing with distributed defects," *J. Meas. Eng.*, vol. 4, no. 2, pp. 87–94, 2016.

[24] A. Nabhan, M. Nouby, A. Sami, and M. Mousa, "Vibration analysis of deep groove ball bearing with outer race defect using ABAQUS," *J. Low Freq. Noise, Vibrat. Act. Control*, vol. 35, no. 4, pp. 312–325, Dec. 2016, doi: 10.1177/0263092316676414.

[25] W. Caesarendra and T. Tjahjowidodo, "A review of feature extraction methods in vibration-based condition monitoring and its application for degradation trend estimation of low-speed slew bearing," *Machines*, vol. 5, no. 4, p. 21, Sep. 2017, doi: 10.3390/machines5040021.

[26] S. S. Nawale and P. D. Kulkarni, "Vibration analysis of ball bearing considering effect of contaminant in lubricant," *Int. J. Sci. Eng. Res.*, vol. 8, no. 4, pp. 170–174, 2017.

[27] K. A. Ibrahim Sheriff, V. Hariharan, and B. Varunesh, "Performance analysis of ball bearing with solid contaminants using vibration analysis," in *Materials, Design, and Manufacturing for Sustainable Environment* (Lecture Notes in Mechanical Engineering). Singapore: Springer, 2021, pp. 175–182, doi: 10.1007/978-981-15-9809-8_14.

[28] M. O. Jakobsen, E. S. Herskind, C. F. Pedersen, and M. B. Knudsen, "Detecting insufficient lubrication in rolling bearings, using a low cost MEMS microphone to measure vibrations," *Mech. Syst. Signal Process.*, vol. 200, Oct. 2023, Art. no. 110553, doi: 10.1016/j.ymssp.2023.110553.

[29] N. Tandon and A. Choudhury, "A review of vibration and acoustic measurement methods for the detection of defects in rolling element bearings," *Tribol. Int.*, vol. 32, no. 8, pp. 469–480, Aug. 1999.

[30] A. M. Al-Ghamd and D. Mba, "A comparative experimental study on the use of acoustic emission and vibration analysis for bearing defect identification and estimation of defect size," *Mech. Syst. Signal Process.*, vol. 20, no. 7, pp. 1537–1571, Oct. 2006, doi: 10.1016/j.ymssp.2004.10.013.

[31] M. Elforjani and D. Mba, "Detecting the onset, propagation and location of non-artificial defects in a slow rotating thrust bearing with acoustic emission," *Insight-Non-Destructive Test. Condition Monitor.*, vol. 50, no. 5, pp. 264–268, May 2008, doi: 10.1784/insi.2008.50.5.264.

[32] S. A. Niknam, V. Songmene, and Y. H. J. Au, "The use of acoustic emission information to distinguish between dry and lubricated rolling element bearings in low-speed rotating machines," *Int. J. Adv. Manuf. Technol.*, vol. 69, nos. 9–12, pp. 2679–2689, Dec. 2013, doi: 10.1007/s00170-013-5222-4.

[33] P. Sachin Krishnan and K. Rameshkumar, "Grinding wheel condition prediction with discrete hidden Markov model using acoustic emission signature," *Mater. Today, Proc.*, vol. 46, pp. 9168–9175, Jan. 2021, doi: 10.1016/j.matpr.2019.12.428.

[34] K. Rameshkumar, R. Sriram, M. Saimurugan, and P. Krishnakumar, "Establishing statistical correlation between sensor signature features and lubricant solid particle contamination in a spur gearbox," *IEEE Access*, vol. 10, pp. 106230–106247, 2022, doi: 10.1109/ACCESS.2022.3210983.

[35] S. A. Mirhadizadeh, E. P. Moncholi, and D. Mba, "Influence of operational variables in a hydrodynamic bearing on the generation of acoustic emission," *Tribol. Int.*, vol. 43, no. 9, pp. 1760–1767, Sep. 2010, doi: 10.1016/j.triboint.2010.03.003.

[36] H. Taura and K. Nakayama, "Behavior of acoustic emissions at the onset of sliding friction," *Tribol. Int.*, vol. 123, pp. 155–160, Jul. 2018, doi: 10.1016/j.triboint.2018.01.025.

[37] K. A. I. Sheriff, V. Hariharan, and T. Kannan, "Analysis of solid contamination in ball bearing through acoustic emission signals," *Arch. Metall. Mater.*, vol. 62, no. 3, pp. 1871–1874, Sep. 2017, doi: 10.1515/amm-2017-0283.

[38] S. Schnabel, S. Golling, P. Marklund, and R. Larsson, "Absolute measurement of elastic waves excited by Hertzian contacts in boundary restricted systems," *Tribol. Lett.*, vol. 65, no. 1, pp. 1–11, Mar. 2017, doi: 10.1007/s11249-016-0790-8.

[39] M. Motahari-Nezhad and S. M. Jafari, "Bearing remaining useful life prediction under starved lubricating condition using time domain acoustic emission signal processing," *Exp. Syst. Appl.*, vol. 168, Apr. 2021, Art. no. 114391, doi: 10.1016/j.eswa.2020.114391.

[40] F. König, C. Sous, A. Ouald Chaib, and G. Jacobs, "Machine learning based anomaly detection and classification of acoustic emission events for wear monitoring in sliding bearing systems," *Tribol. Int.*, vol. 155, Mar. 2021, Art. no. 106811, doi: 10.1016/j.triboint.2020.106811.

[41] S. Poddar and N. Tandon, "Detection of particle contamination in journal bearing using acoustic emission and vibration monitoring techniques," *Tribol. Int.*, vol. 134, pp. 154–164, Jun. 2019, doi: 10.1016/j.triboint.2019.01.050.

[42] S. Poddar and N. Tandon, "Classification and detection of cavitation, particle contamination and oil starvation in journal bearing through machine learning approach using acoustic emission signals," *Proc. Inst. Mech. Eng., J, J. Eng. Tribol.*, vol. 235, no. 10, pp. 2137–2143, 2021, doi: 10.1177/1350650121991316.

[43] B. Scheeren, M. L. Kaminski, and L. Pahlavan, "Acoustic emission monitoring of naturally developed damage in large-scale low-speed roller bearings," *Struct. Health Monitor.*, vol. 23, no. 1, pp. 360–382, Jan. 2024, doi: 10.1177/14759217231164912.

[44] I. Y. Önel, K. B. Dalci, and I. Senol, "Detection of outer raceway bearing defects in small induction motors using stator current analysis," *Sadhana*, vol. 30, no. 6, pp. 713–722, Dec. 2005, doi: 10.1007/bf02716705.

[45] A. Alwodai, T. Wang, Z. Chen, F. Gu, R. Cattley, and A. Ball, "A study of motor bearing fault diagnosis using modulation signal bispectrum analysis of motor current signals," *J. Signal Inf. Process.*, vol. 4, no. 3, pp. 72–79, 2013, doi: 10.4236/jsip.2013.43b013.

[46] T. Maruyama, M. Maeda, and K. Nakano, "Lubrication condition monitoring of practical ball bearings by electrical impedance method," *Tribol. Online*, vol. 14, no. 5, pp. 327–338, 2019, doi: 10.2474/trol.14.327.

[47] H. Nakamura and Y. Mizuno, "Diagnosis for slight bearing fault in induction motor based on combination of selective features and machine learning," *Energies*, vol. 15, no. 2, p. 453, Jan. 2022, doi: 10.3390/en15020453.

[48] K. Adamsab, "Machine learning algorithms for rotating machinery bearing fault diagnostics," *Mater. Today, Proc.*, vol. 44, pp. 4931–4933, Jan. 2021, doi: 10.1016/j.matpr.2020.12.050.

[49] B. Samanta, K. R. Al-Balushi, and S. A. Al-Araimi, "Artificial neural networks and support vector machines with genetic algorithm for bearing fault detection," *Eng. Appl. Artif. Intell.*, vol. 16, nos. 7–8, pp. 657–665, Oct. 2003, doi: 10.1016/j.engappai.2003.09.006.

[50] S. Zhang, S. Zhang, B. Wang, and T. G. Habetler, "Deep learning algorithms for bearing fault diagnostics—A comprehensive review," *IEEE Access*, vol. 8, pp. 29857–29881, 2020, doi: 10.1109/ACCESS.2020.2972859.

[51] O. Abdeljaber, S. Sassi, O. Avci, S. Kiranyaz, A. A. Ibrahim, and M. Gabbouj, "Fault detection and severity identification of ball bearings by online condition monitoring," *IEEE Trans. Ind. Electron.*, vol. 66, no. 10, pp. 8136–8147, Oct. 2019, doi: 10.1109/TIE.2018.2886789.
[52] M. Bhadane and K. I. Ramachandran, "Bearing fault identification and classification with convolutional neural network," in *Proc. Int. Conf. Circuit, Power Comput. Technol. (ICCPCT)*, Apr. 2017, pp. 1–5, doi: 10.1109/ICCPCT.2017.8074401.
[53] J. Koshy, N. K. Prakash, and T. Ananthan, "Wavelet based bearing fault prognosis using machine learning in cloud platform," in *Proc. Int. Conf. Ind. 4.0 Technol.*, Sep. 2022, pp. 1–7, doi: 10.1109/I4Tech55392.2022.9952792.
[54] Q. Ni, J. C. Ji, and K. Feng, "Data-driven prognostic scheme for bearings based on a novel health indicator and gated recurrent unit network," *IEEE Trans. Ind. Informat.*, vol. 19, no. 2, pp. 1301–1311, Feb. 2023, doi: 10.1109/TII.2022.3169465.
[55] J. M. Wakiru, L. Pintelon, P. N. Muchiri, and P. K. Chemweno, "A review on lubricant condition monitoring information analysis for maintenance decision support," *Mech. Syst. Signal Process.*, vol. 118, pp. 108–132, Mar. 2019, doi: 10.1016/j.ymssp.2018.08.039.
[56] M. H. Rahman, S. Shahriar, and P. L. Menezes, "Recent progress of machine learning algorithms for the oil and lubricant industry," *Lubricants*, vol. 11, no. 7, p. 289, Jul. 2023, doi: 10.3390/lubricants11070289.
[57] V. Sugumaran and K. I. Ramachandran, "Effect of number of features on classification of roller bearing faults using SVM and PSVM," *Exp. Syst. Appl.*, vol. 38, no. 4, pp. 4088–4096, Apr. 2011, doi: 10.1016/j.eswa.2010.09.072.
[58] N. Senthilnathan, T. N. Babu, K. S. D. Varma, S. Rushmith, J. A. Reddy, K. V. N. Kavitha, and D. R. Prabha, "Recent advancements in fault diagnosis of spherical roller bearing: A short review," *J. Vibrat. Eng. Technol.*, vol. 12, no. 4, pp. 6963–6977, Apr. 2024, doi: 10.1007/s42417-024-01293-4.
[59] P. K. Sahu, "Grease contamination detection in the rolling element bearing using deep learning technique," *Int. J. Mech. Eng. Robot. Res.*, vol. 11, no. 4, pp. 275–280, 2022, doi: 10.18178/ijmerr.11.4.275-280.
[60] Y. Zhao, X. Wang, S. Han, J. Lin, and Q. Han, "Fault diagnosis for abnormal wear of rolling element bearing fusing oil debris monitoring," *Sensors*, vol. 23, no. 7, p. 3402, Mar. 2023, doi: 10.3390/s23073402.
[61] K. Kira and L. A. Rendell, "A practical approach to feature selection," in *Proc. 9th Int. Work. Mach. Learn.*, 1992, pp. 249–256, doi: 10.1016/B978-1-55860-247-2.50037-1.
[62] P. Krishnakumar, K. Rameshkumar, and K. I. Ramachandran, "Feature level fusion of vibration and acoustic emission signals in tool condition monitoring using machine learning classifiers," *Int. J. Prognostics Health Manag.*, vol. 9, no. 1, pp. 1–15, Nov. 2020, doi: 10.36001/ijphm.2018.v9i1.2694.
[63] J. R. Quinlan, "Induction of decision trees," *Mach. Learn.*, vol. 1, no. 1, pp. 81–106, Mar. 1986, doi: 10.1007/bf00116251.
[64] A. D. Gordon, L. Breiman, J. H. Friedman, R. A. Olshen, and C. J. Stone, "Classification and regression trees," *Biometrics*, vol. 40, no. 3, p. 874, Sep. 1984, doi: 10.2307/2530946.
[65] L. Breiman, "Bagging predictors," *Mach. Learn.*, vol. 24, no. 2, pp. 123–140, Aug. 1996, doi: 10.1007/bf00058655.
[66] C. Cortes and V. Vapnik, "Support-vector networks," *Mach. Learn.*, vol. 20, no. 3, pp. 273–297, Sep. 1995, doi: 10.1007/bf00994018.
[67] M. Sokolova and G. Lapalme, "A systematic analysis of performance measures for classification tasks," *Inf. Process. Manag.*, vol. 45, no. 4, pp. 427–437, Jul. 2009, doi: 10.1016/j.ipm.2009.03.002.

K. RAMESHKUMAR received the B.E. degree in mechanical engineering and the M.E. degree in production engineering, in 1990 and 1991, respectively, and the Ph.D. degree in optimization of discrete and continuous optimization problems using bio-inspired algorithms from the PSG College of Technology, Bharathiar University, Coimbatore, India, in 2008. Later, he was with the projects department in a staple fiber manufacturing plant in India and was involved in the erection, commissioning, and technical services of a 150 TPD viscose staple fiber manufacturing plant in collaboration with M/s Lenzing, Austria. He was also a Faculty Member with the Department of Engineering, Ministry of Manpower, Higher College of Technology, Oman, from 2009 to 2010 and from 2015 to 2016. He is currently a Professor and the Chairperson with the Department of Mechanical Engineering, Amrita School of Engineering, Amrita Vishwa Vidyapeetham, Coimbatore Campus. His current activities include administration of the Mechanical Engineering Department, teaching B.Tech., M.Tech., and Ph.D. level courses, coordinating OBE and NBA activities of the department, and guiding student research projects (UG, PG, and Ph.D.) in predictive analytics of machine tools using machine learning algorithms, tool condition monitoring, weld condition monitoring, machining dynamics, multi-objective optimization, and discrete event simulation of manufacturing systems. He has received research grants from government agencies, namely AICTE, DRDO, AR&DB, and DST. He received the Amrita University Chancellor's Publication Award, in 2020 and 2023.

KAVIARASU NATARAJ received the bachelor's degree in mechanical engineering from Anna University, India, and the M.Tech. degree in engineering design from the Department of Mechanical Engineering, Amrita School of Engineering, Amrita Vishwa Vidyapeetham, Coimbatore Campus, India, in 2020. He is currently working at M/s Taark Equipments Pvt. Ltd., Pollachi, Coimbatore, as a Senior Design Engineer.

P. KRISHNAKUMAR received the bachelor's degree in mechanical engineering from Bharathiar University, India, the M.Tech. degree in computer integrated manufacturing from the PSG College of Technology, India, in 2000, and the Ph.D. degree in mechanical engineering from the Amrita School of Engineering, Amrita Vishwa Vidyapeetham, Coimbatore Campus, India, in 2017. He is currently an Associate Professor and the Dy. COE with the Department of Mechanical Engineering, Amrita School of Engineering, Amrita Vishwa Vidyapeetham, Coimbatore Campus. He received sponsored projects in metal cutting and machine condition monitoring from AR&DB, DRDO, and DST. His research interests include design and analysis, metal cutting, and micro-machining. He received the Amrita University Chancellor's Publication Award, in 2023.

M. SAIMURUGAN received the B.E. degree in mechanical engineering from Bharathiar University, Coimbatore, India, in 1998, the M.E. degree in computer-aided design from Periyar University, India, in 2000, and the Ph.D. degree in mechanical engineering from the Amrita School of Engineering, Amrita Vishwa Vidyapeetham, Coimbatore Campus, India, in 2013. He is currently an Associate Professor with the Department of Mechanical Engineering, Amrita School of Engineering, Amrita Vishwa Vidyapeetham, Coimbatore Campus. He received sponsored projects in machine condition monitoring from AR&DB, DRDO, and DST. His research interests include vibration analysis, machine learning, and machine condition monitoring. His research articles were the best papers at the 12th IEEE India International Conference on Electronics, Energy, Environment, Communication, Computer Science, Control (INDICON, 2015) and the International Conference on Soft Computing in Applied Sciences and Engineering, in 2015. He also received the Amrita University Chancellor's Publication Award, in 2023.